A Region of Intense Plasma Wave Turbulence on Auroral Field Lines

D. A. GURNETT[1]

Max-Planck-Institut für extraterrestrische Physik, 8046 Garching/Munich, West Germany

L. A. FRANK

Department of Physics and Astronomy, University of Iowa, Iowa City, Iowa 52242

Plasma wave measurements from the Hawkeye 1 and Imp 6 satellites show that a broad region of intense plasma wave turbulence occurs on the high-latitude auroral field lines at altitudes ranging from a few thousand kilometers in the ionosphere to many earth radii in the distant magnetosphere. This turbulence occurs in an essentially continuous band on the auroral L shells at all local times around the earth and is most intense during periods of auroral activity. The electric field intensity of this turbulence is often quite large, with maximum field strengths of about 10 mV m^{-1} and peak intensities in the frequency range 10–50 Hz. Magnetic field perturbations indicative of field-aligned currents and weak bursts of whistler mode magnetic noise are also observed in the same region as the electric field turbulence. In the local afternoon and evening the electric field turbulence is closely associated with V-shaped auroral hiss emissions. In some cases the electric field turbulence appears as a lowering and intensification of the low-frequency portion of the auroral hiss spectrum. Comparisons with plasma measurements and with similar measurements from other satellites strongly suggest that this plasma wave turbulence occurs on magnetic field lines which connect with regions of intense inverted V electron precipitation at low altitudes and with regions of intense earthward plasma flow in the distant magnetotail. The plasma instabilities which could produce this turbulence and the possible role which this turbulence may play in the heating and acceleration of the auroral particles are considered.

INTRODUCTION

Recent studies of plasma wave measurements obtained from the Hawkeye 1 and Imp 6 satellites have revealed the existence of a broad region of plasma wave turbulence on auroral field lines at altitudes ranging from a few thousand kilometers in the auroral ionosphere to many earth radii in the distant magnetosphere. The electric field intensity of this turbulence is often quite large, with maximum field strengths of about 10 mV m^{-1}. The frequency range of the electric field noise typically extends from about 10 Hz to several kilohertz, the maximum intensity occurring at about 10–50 Hz. The electric field turbulence sometimes appears to be closely associated with whistler mode auroral hiss emissions which are frequently observed on the high-latitude auroral field lines. Weak bursts of magnetic noise are also detected in the same region as the electric field turbulence, although these magnetic noise bursts do not appear to be directly associated with the electric field noise. In this paper we present a detailed study of the plasma wave turbulence observed by Hawkeye 1 and Imp 6 on high-latitude auroral field lines, and we investigate the relationship of this turbulence to magnetic field and plasma measurements obtained in the same region.

The importance of studying plasma wave turbulence on auroral field lines arises from the possible role that this turbulence may play in producing regions of 'anomalous' resistivity in the field-aligned currents which flow between the auroral oval and the distant magnetosphere. For many years it has been suggested [*Sagdeev and Galeev*, 1966] that intense electric fields produced by current-driven instabilities can interact with the current-carrying particles to produce an effective resistivity many orders of magnitude larger than the resistivity produced by Coulomb collisions. *Kindel and Kennel* [1971] have considered the possible current-driven instabilities which could occur in the auroral zone and have concluded that the electrostatic ion cyclotron and ion acoustic modes should be unstable in the regions of field-aligned currents associated with the auroral electron precipitation. If the electric field turbulence produced by these instabilities grows to sufficiently large amplitudes, the associated anomalous resistivity can produce large potential differences of several kilovolts along the magnetic field in these regions. Several investigators, including *Coroniti and Kennel* [1972, 1973], *Sato and Holzer* [1973], *Holzer and Sato* [1973], *Papadopoulos and Coffey* [1974], *Mozer* [1977], and others, have considered the possibility that the resulting parallel electric field could accelerate runaway electrons to energies of several keV, thereby accounting for the intense electron precipitation commonly observed in the auroral regions. Since other turbulence free acceleration mechanisms have also been proposed [*Carlqvist*, 1972], it is of considerable importance to establish whether intense electric field turbulence occurs in the regions of field-aligned current associated with the auroral electron precipitation.

Scarf et al. [1973, 1975] have previously reported observations of electrostatic plasma wave turbulence associated with field-aligned currents for a few cases in which the Ogo 5 spacecraft reached sufficiently high magnetic latitudes to obtain measurements on auroral field lines, at $L \simeq 7$–8, in the region close to the earth. During magnetically disturbed periods in the local afternoon and evening the electrostatic turbulence detected by Ogo 5 usually consisted of a few abrupt transient bursts with frequencies extending from about 1 kHz to about 10 kHz and with durations of a few seconds. The individual bursts tended to correlate with gradients in the magnetic field caused by field-aligned currents. *Scarf et al.* [1972] and *Fredricks et al.* [1973] discussed similar observations of enhanced electrostatic wave turbulence detected by Ogo 5 at the boundaries of the dayside polar cusp.

In comparison with the Ogo 5 results, both the Hawkeye 1 and the Imp 6 spacecraft provide measurements at higher

[1] Permanent address: Department of Physics and Astronomy, University of Iowa, Iowa City, Iowa 52242.

Paper number 6A0737.

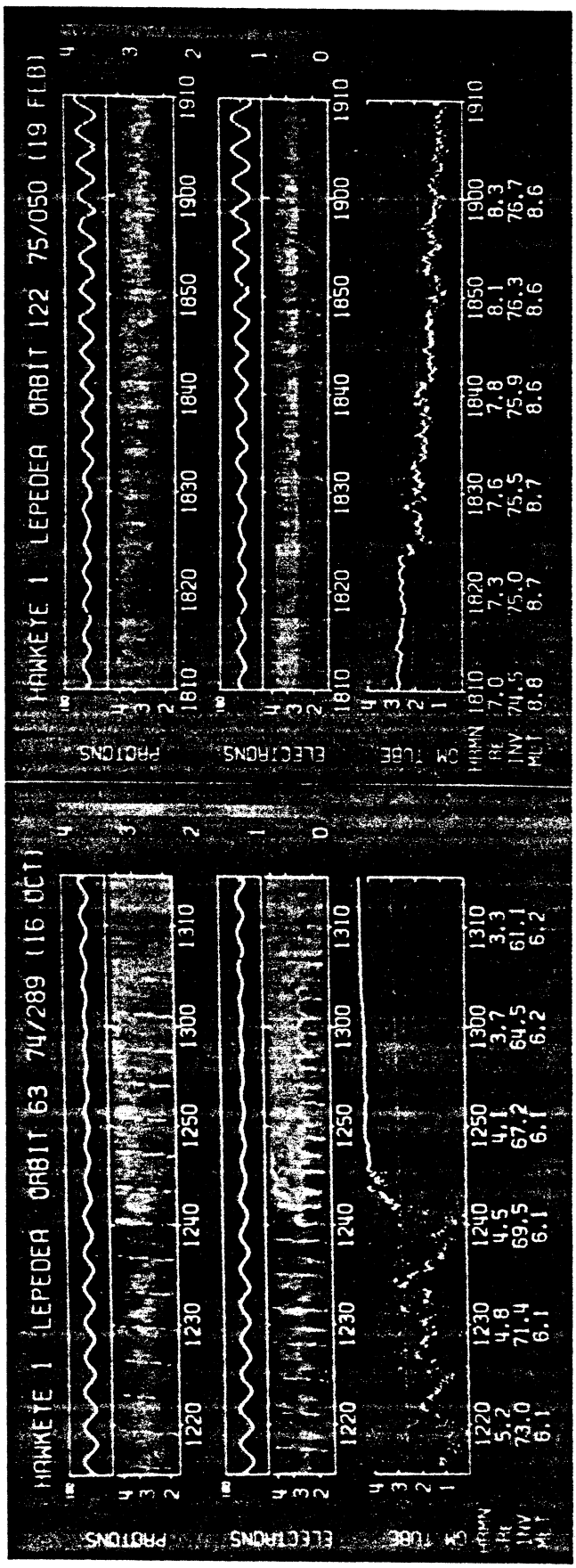

Plate 1. The Lepedea and GM tube data for the inbound Hawkeye 1 pass in Figure 2. The two spectrograms display the color-coded responses of the Lepedea as functions of the logarithm to the base 10 of the energy (ordinate) and universal time (abscissa). The color bar at the right-hand side of the figure displays the color coding ($\log_{10}$ of the analyzer responses). Each spectrogram is topped with a plot of the instantaneous pitch angles as determined with the on-board magnetometer. The most intense broad-band electrostatic noise and magnetic noise bursts occur from about 1234 to 1244, just before the rapid increase in the GM tube counting rate and in a region characterized by low-energy magnetosheathlike proton intensities.

Plate 2. The Lepedea and GM tube data for the inbound Hawkeye 1 pass in Figure 3. The onset of the broad-band electrostatic noise and magnetic noise bursts and the cutoff of the continuum radiation at 13.3 kHz occur as the spacecraft enters the region of low energy after about 1825 UT.

magnetic latitudes than were possible with Ogo 5. In this study it is therefore possible to obtain a much more comprehensive survey of phenomena occurring on auroral field lines at all local times and for both quiet and magnetically disturbed conditions. The plasma wave instrumentation on Hawkeye 1 and Imp 6 also provides measurements over a broader frequency range, particularly at lower frequencies, and with greater electric field sensitivity. As will be shown, the electric field turbulence detected by Hawkeye 1 and Imp 6 differs considerably from the Ogo 5 results. The electric field turbulence occurs with a relatively steady intensity over a broad region for a substantial fraction of the time (20–50%), rather than a few intense bursts, and the most intense component of the noise occurs at frequencies well below the lower frequency limit of the Ogo 5 electric field experiment.

Spacecraft Orbits and Experiment Descriptions

To aid in interpreting the measurements presented in this paper, we briefly describe the orbits of Hawkeye 1 and Imp 6 and the regions of the magnetosphere sampled by these two satellites. Hawkeye 1 is in a highly eccentric polar orbit with initial perigee and apogee geocentric radial distances of 6,847 km and 130,856 km, respectively. The apogee is located almost directly over the north pole, so Hawkeye 1 provides extensive coverage of the high-latitude region of the magnetosphere. Since the region of primary interest for this study is relatively close to the earth ($R \lesssim 10\ R_E$), the coordinates used throughout this paper are the magnetic latitude λ_m, the magnetic local time MLT, and the geocentric radial distance R. A typical magnetic meridional plane (R, λ_m) trajectory of Hawkeye 1 is shown in Figure 1. Because of the 11° tilt of the earth's magnetic dipole axis and the long-term secular changes in the orbit, measurements can be obtained over a broad range of magnetic latitudes if a sufficiently large quantity of data is used. For this study we have used Hawkeye 1 data from a period of approximately 14 months starting at launch on June 3, 1974, and continuing until August 29, 1975. The shaded area labeled 'Region sampled by Hawkeye 1' in Figure 1 indicates the region of the magnetic meridian plane sampled by Hawkeye 1 for a representative range of magnetic local times (2300–0100) near local midnight. In the northern hemisphere, Hawkeye 1 provides measurements on a typical auroral field line ($L = 8$) at radial distances ranging from about 4 to 6 R_E. In the southern hemisphere, measurements are obtained at radial distances ranging from about 1.1 to 1.8 R_E. Because of the increasing perigee altitude, data obtained during later periods of operation will extend the measurements on auroral field lines in the southern hemisphere to altitudes of about 2.6 R_E, so that eventually, observations will be provided over a very wide range of altitudes. The data set currently available for this study, however, has a distinct gap in the altitude coverage (at $L = 8$) from about 1.8 to 4.0 R_E.

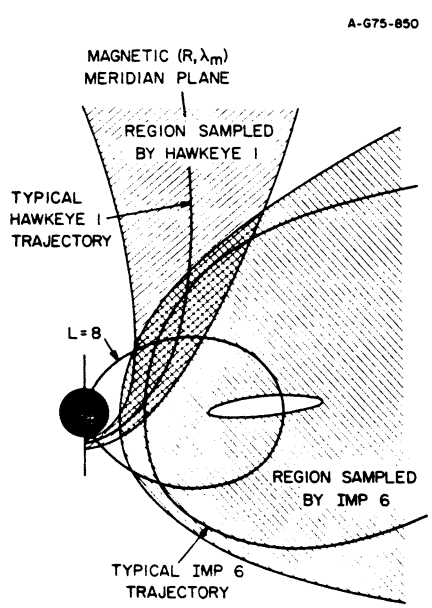

Fig. 1. Typical trajectories and the boundaries of the region sampled by Hawkeye 1 and Imp 6 in the magnetic meridional plane (geocentric radial distance and magnetic latitude coordinates). Secular changes in the orbit provide coverage over a wide range of magnetic latitudes. The measurements analyzed include 14 months of data from Hawkeye 1 and 3.5 years of data from Imp 6.

The Imp 6 spacecraft is in a highly eccentric orbit with initial perigee and apogee geocentric radial distances of 6,613 and 212,630 km, respectively. In contrast to the Hawkeye 1 orbit the apogee of Imp 6 is located at a low latitude, close to the equatorial plane of the earth. However, the inclination of the orbit plane is sufficiently large to provide measurements at relatively high magnetic latitudes, up to about 55°, in the region near the earth. A typical magnetic meridian plane trajectory for Imp 6 is shown in Figure 1. As with Hawkeye 1, the tilt of the earth's magnetic dipole axis and orbital perturbations greatly extend the range of magnetic latitudes at low altitudes which are sampled during the lifetime of the spacecraft. For this study we have analyzed all of the available telemetry during the 3.5-year lifetime of Imp 6, from March 13, 1971, to October 1, 1974. The region of the magnetic meridional plane sampled by Imp 6 during this period is shown in Figure 1 for a representative range of magnetic local times (2300–0100) near local midnight. It is evident from Figure 1 that the Hawkeye 1 and Imp 6 spacecraft together provide coverage over a very broad region. The detailed coverage tends to vary somewhat with local time, but in general, along the auroral field lines, all altitudes above about 4 R_E are sampled by these two spacecraft. In some local time ranges a small hole in the coverage occurs near the magnetic equator at radial distances of about 4–5 R_E. This small hole in the coverage is not particularly relevant for the region of interest in this study.

Since the details of both the Hawkeye 1 and the Imp 6 plasma wave experiment have been described in previous reports [*Kurth et al.*, 1975; *Gurnett and Shaw*, 1973], only a few brief comments are made concerning the plasma wave instrumentation. Both experiments use long electric antennas, 42.45 m from tip to tip for Hawkeye 1 and 92.5 m from tip to tip for Imp 6. Magnetic field measurements are obtained from a search coil antenna on Hawkeye 1 and from a single turn loop antenna on Imp 6. The frequency range of the Hawkeye 1 instrumentation, 1.78 Hz to 178 kHz, is somewhat larger than the frequency range of the Imp 6 instrumentation, 36 Hz to 178 kHz. Both experiments provide electric field intensities in 16 frequency channels, extending with an approximately constant fractional frequency spacing over the entire frequency range, and wide-band wave form measurements for high-resolution frequency-time spectrograms.

Plasma measurements were acquired with an electrostatic analyzer, a low-energy proton and electron differential energy analyzer (Lepedea) [cf. *Frank*, 1967], on board Hawkeye 1. Directional differential intensities of positive ions and electrons over the energy range 50 eV $\leq E \leq$ 40 keV are telemetered for directions perpendicular to the spacecraft spin

axis. A collimated thin-windowed Geiger-Mueller (GM) tube was employed for determining directional intensities of electrons with $E > 45$ keV.

The Hawkeye 1 magnetometer is a three-orthogonal-axis flux gate instrument constructed by the Schonstedt Instrument Company. The sensor package is mounted at the end of a boom 1.22 m from the closest face of the spacecraft and 1.57 m from its rotational axis. The magnetometer has four sensitivity ranges on each axis, selectable by ground command: ±150, ±450, ±1,500, and ±25,000 γ. Instrumental accuracy is ±0.5% of full range on each axis in each range. The frequency response is flat from 0 to 1 Hz and down 3 dB at 10 Hz, rolling off at higher frequencies at 6 dB/octave. The analog outputs of the three axes are sampled simultaneously, at approximately equal intervals of 1.92 s, with 8-bit resolution.

Some Representative Plasma Wave Observations at High Latitudes

To illustrate the main characteristics of the plasma wave observations obtained by Hawkeye 1 and Imp 6 on the auroral L shells, we first discuss four typical passes through the high-latitude region of the magnetosphere. These passes, which are shown in Figures 2–5, were selected to illustrate the variety of plasma wave phenomena detected in this region at various local times. The data in Figures 2, 3, and 4 are from Hawkeye 1 passes in the local dawn, local morning, and local afternoon,

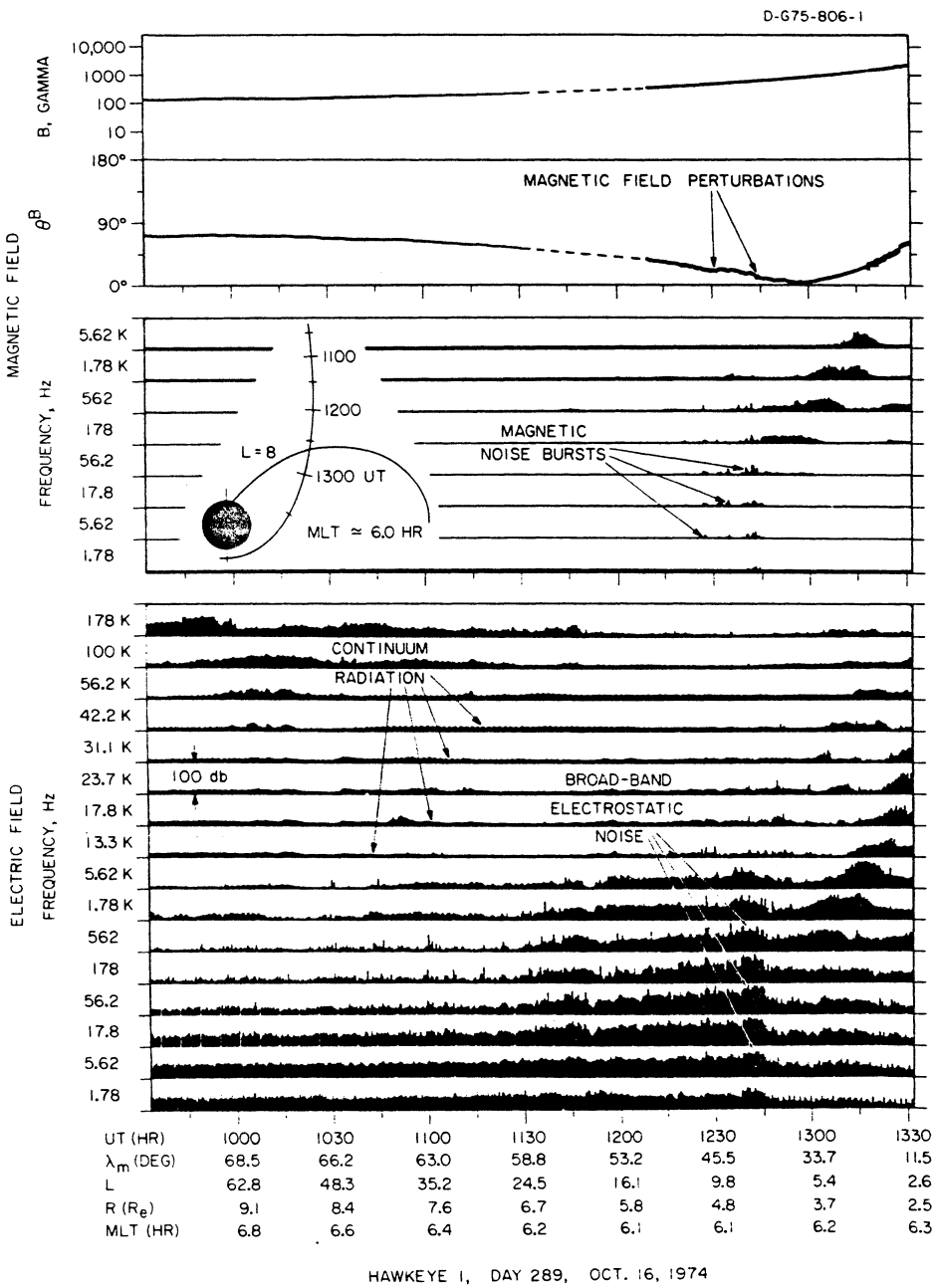

Fig. 2. A representative Hawkeye 1 pass near local dawn. A region of intense broad-band electrostatic noise and magnetic noise bursts is evident from about 1225 to 1244 UT. Perturbations in the magnetic field direction θ^B indicate the presence of field-aligned currents in this region.

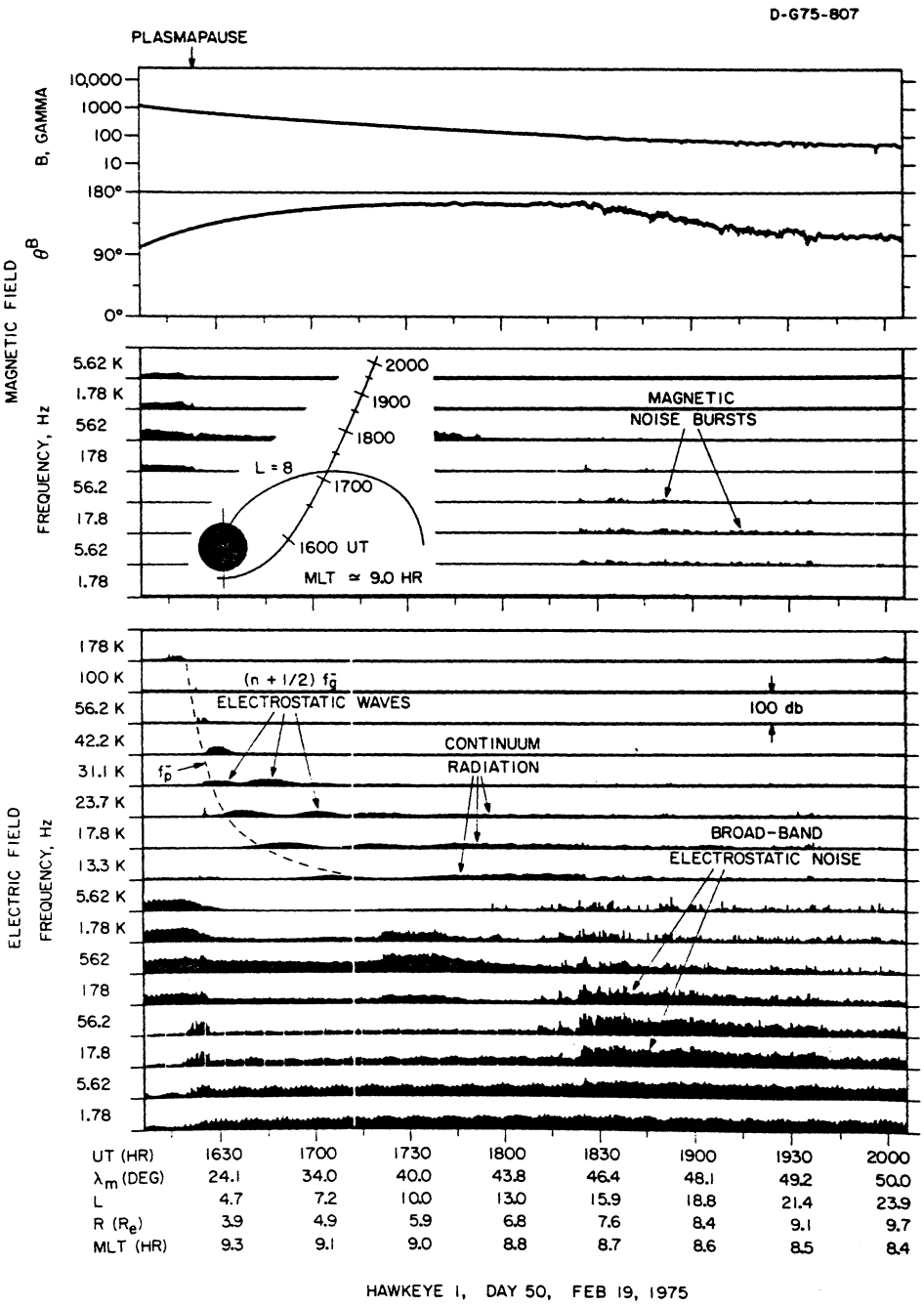

Fig. 3. A representative Hawkeye 1 pass at local morning. A broad region of intense broad-band electrostatic noise and magnetic noise bursts is evident from about 1825 to 1940 UT, which accompanies a distinct skewing in the magnetic field direction and magnetic fluctuations. The distinct cutoff in the continuum radiation at about 1825 UT indicates an abrupt increase in the plasma density at this time.

respectively, and the data in Figure 5 are from an Imp 6 pass near local midnight. The top panel of each illustration shows the magnetic field magnitude and direction, and the center and bottom panels show the plasma wave magnetic and electric field intensities. The angle θ^B in Figures 2, 3, and 4 is the angle between the magnetic field and spacecraft spin axis, and the angle $\varphi_{SM}{}^B$ in Figure 5 is the azimuthal direction of the magnetic field in solar magnetospheric coordinates. Because of a failure in the Hawkeye 1 attitude determination system after 3 months in flight, θ^B is the only magnetic field orientation angle that is available at present for the periods shown in Figures 2, 3, and 4. (This shortcoming is being remedied in subsequent work using data from the scientific instruments themselves to reconstruct the spacecraft attitude.) The wave magnetic field intensities are shown in 8 frequency channels, from 1.78 Hz to 5.62 kHz for Hawkeye 1 and from 36.0 Hz to 1.78 kHz for Imp 6, and the electric field intensities are shown in 16 frequency channels, from 1.78 Hz to 178 kHz for Hawkeye 1 and from 36.0 Hz to 178 kHz for Imp 6. The intensity scale for each channel is proportional to the logarithm of the field strength, with a range of 100 dB from the base line of one channel to the base line of the next higher channel. For the Hawkeye 1 measurements, every sample is plotted. For the Imp 6 data the dots give the peak field strengths, and the vertical bars give the average field strengths over intervals of 81.92 s.

The first representative pass (in Figure 2) is an inbound

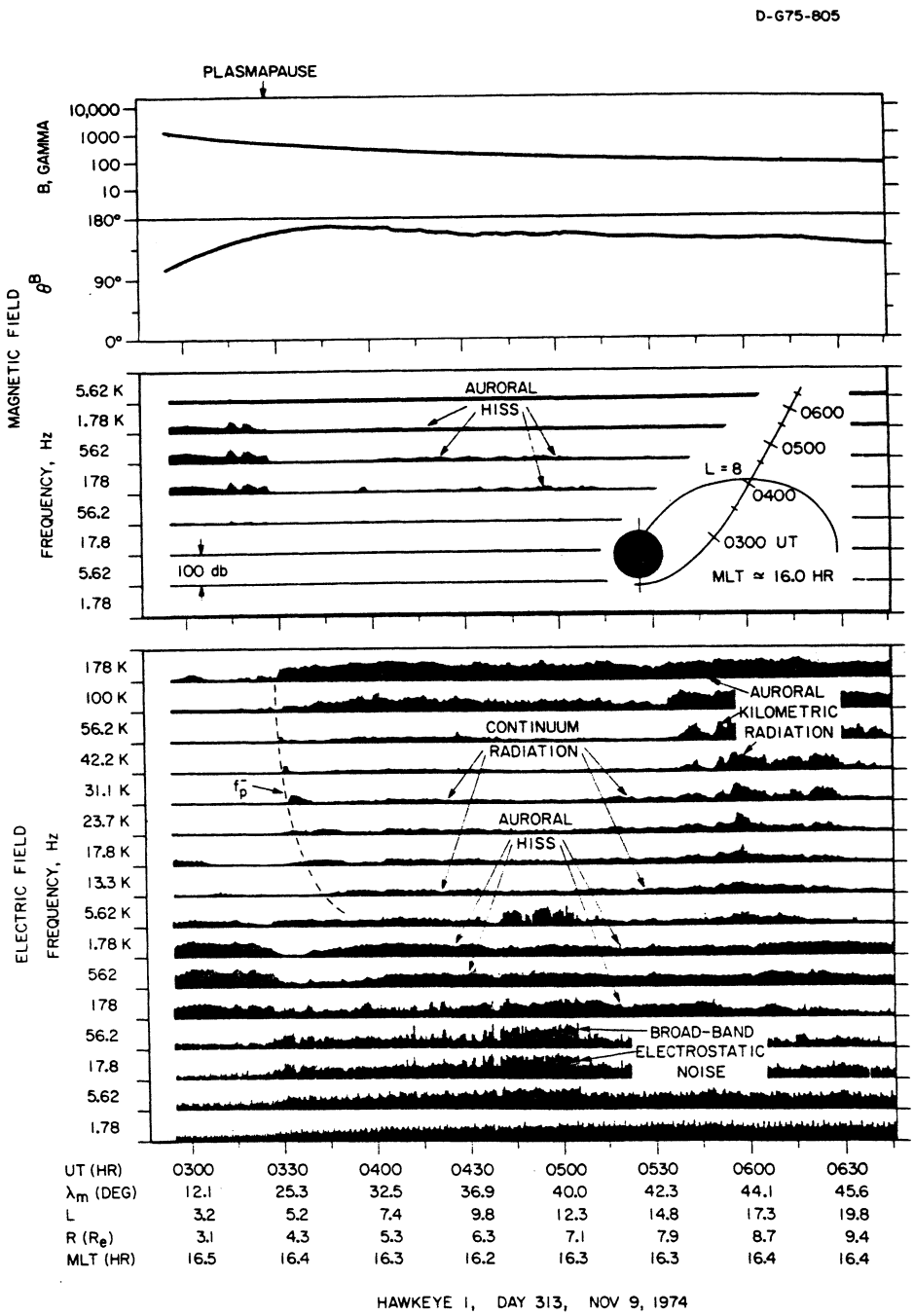

Fig. 4. A representative Hawkeye 1 pass at local afternoon. The broad-band electrostatic noise in this case occurs centered on a region of auroral hiss emission, similar to Figure 14. No magnetic noise bursts are detected during this pass.

Hawkeye 1 pass near local dawn at about 0600 magnetic local time. The spacecraft trajectory in the magnetic meridian plane (R, λ_m coordinates) for this pass is shown by the small sketch in the center panel of Figure 2. Several types of plasma wave emissions are present during this pass. In the high-frequency (13.3–178 kHz) electric field channels, two types of electromagnetic emissions called auroral kilometric radiation and continuum radiation [*Gurnett*, 1974, 1975] are detected throughout most of this pass. These electromagnetic emissions occur at frequencies above the local plasma frequency and are generated in regions of higher plasma density near the earth. Deep within the magnetosphere, at L values less than 4, plasmaspheric hiss [*Russell et al.*, 1969] is evident in both the electric and the magnetic field channels at frequencies from about 562 Hz to 5.62 kHz, increasing in frequency toward lower L values. At lower frequencies, from about 5.62 Hz to 1.78 kHz, a region of very intense electric field noise can be seen from about 1145 to 1245 UT. The intensity of this noise increases gradually with decreasing radial distance and reaches peak intensity in the 17.8- and 56.2-Hz channels at about 1240 UT ($L \simeq 8.1$), followed by a very abrupt decrease in the intensity at about 1244 UT. At the time of maximum intensity this noise is very intense, with a broad-band rms electric field strength of 10.8 mV m^{-1} and a peak intensity of about 35 mV m^{-1}. Since this noise occurs over a broad range of frequencies and is most evident in the electric field data, we refer to this noise as broad-band electrostatic noise. This name is the same as was used for a similar type of noise detected by the Imp 8

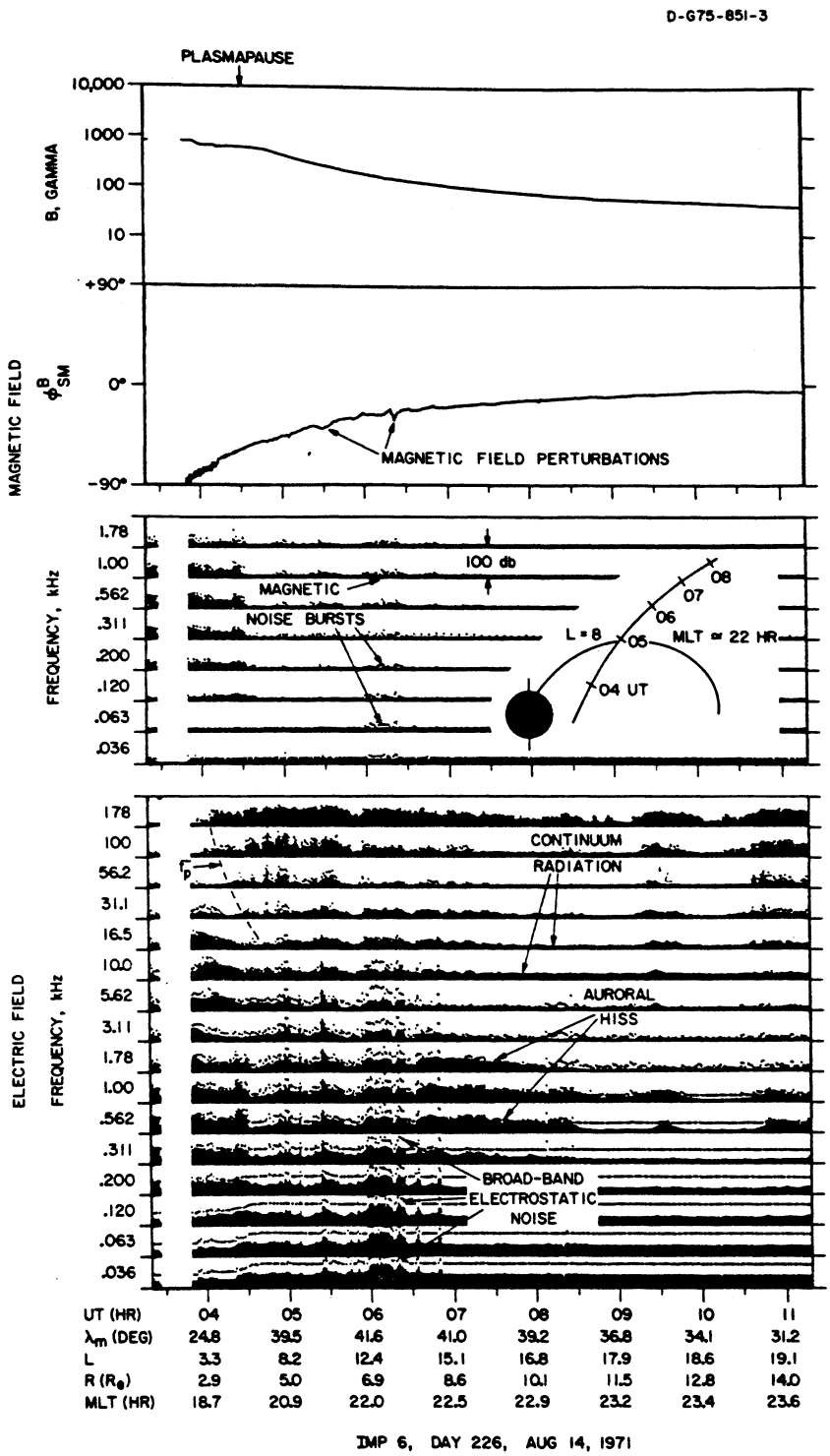

Fig. 5. A representative Imp 6 pass, again at local evening. The dots and vertical bars give the peak and average field intensities, respectively. The broad-band electrostatic noise is very intense in the low-frequency electric field channels, ≤120 Hz, and extends with detectable intensities to frequencies above 10 kHz.

spacecraft in the distant magnetotail [*Gurnett et al.*, 1976]. As will be discussed later, these two types of noise are believed to be essentially identical, which justifies the use of the same terminology, although this association remains a matter of later interpretation. The term electrostatic is used because, as will be shown, the electric to magnetic field ratio is much larger than would be expected for any of the usual electromagnetic modes which occur in a plasma. Broad-band electrostatic noise of the type shown in Figure 2 is frequently detected by Hawkeye 1 and Imp 6 on the high-latitude auroral field lines and is the main topic of this paper.

In the same region as the broad-band electrostatic noise, numerous bursts of low-frequency (1.78–562 Hz) magnetic field noise are also evident in Figure 2. As will be shown, the spectrum of these magnetic noise bursts is distinctly different from the spectrum of the broad-band electrostatic noise. The temporal variations are also quite different. The magnetic noise usually consists of many short transient bursts, whereas

the broad-band electrostatic noise has a more nearly constant amplitude. Thus even though both types of noise occur in the same region and in the same general frequency range, these emissions apparently consist of two distinctly different plasma instabilities. In this paper the low-frequency magnetic noise of the type shown in Figure 2 will be called magnetic noise bursts.

The second representative pass (Figure 3) is an outbound Hawkeye 1 pass in the local morning at about 0900 MLT. No auroral kilometric radiation is detectable in the high-frequency electric field channels during this pass. A very weak level of continuum radiation is evident in the 13.3- to 23.7-kHz channels at radial distances beyond about 6.0 R_E. In the region beyond the plasmapause, after about 1555 UT, several distinct noise bands are evident, sweeping downward in frequency from about 56.2 to 13.3 kHz. These noise bands are $(n + \frac{1}{2})f_g^-$ electrostatic cyclotron harmonic emissions of the type discussed by *Shaw and Gurnett* [1975]. As indicated by the dashed line in Figure 3, the local electron plasma frequency f_p^- can be estimated from the frequency at which these emissions occur. Inside the plasmapause, before about 1555 UT, plasmaspheric hiss is evident in both the electric and the magnetic field channels from about 178 Hz to 5.62 kHz. Starting at about 1825 UT and extending to about 1940 UT, a region of intense broad-band electrostatic noise is evident, with characteristics very similar to the example in Figure 2. In this same region, many distinct magnetic noise bursts are also clearly evident in the low-frequency (1.78–178 Hz) magnetic field channels.

The third representative pass (Figure 4) is an outbound Hawkeye 1 pass in the local afternoon at about 1600 magnetic local time. The plasma wave activity during this pass is more complicated than that for the two preceding examples. In the high-frequency electric field channels, above about 10 kHz, very high intensities of auroral kilometric radiation are present throughout most of this pass. At the plasmapause, which is located at about 0330 UT, an abrupt cutoff is evident in the auroral kilometric radiation. This cutoff occurs when the local electron plasma frequency f_p^- exceeds the wave frequency. In this same region, some rather poorly defined $(n + \frac{1}{2})f_g^-$ electron cyclotron harmonics, similar to those in Figure 3, can be seen sweeping downward in frequency near the electron plasma frequency, indicated by the dashed lines in Figure 4. Beyond the plasmapause, continuum radiation can be seen extending down to frequencies of about 5 kHz. Although not evident in Figure 4, the wide-band wave form data show a distinct low-frequency cutoff at a frequency which varies from about 5 kHz at 0430 UT to about 2 kHz at 0600 UT. This cutoff has been used to estimate the electron plasma frequency in this region, as indicated in Figure 4. At slightly lower frequencies, in the 178-Hz to 1.78-kHz channels, a relatively steady band of noise is evident, extending over a broad region beyond about 0345 UT. On the basis of detailed examinations of high-resolution spectrograms of the wide-band wave form data, as will be discussed in a later section, this noise is identified as auroral hiss, a type of whistler mode emission which is commonly observed in the auroral zone by low-altitude satellites [*Gurnett*, 1966; *Laaspere et al.*, 1971; *Gurnett and Frank*, 1972*a*]. The magnetic field of the auroral hiss is also evident in the corresponding magnetic field channels. At even lower frequencies, in the 17.8- and 56.2-Hz electric field channels, a distinct enhancement can be seen in the electric field intensity from about 0437 to 0505 UT. This noise is identified as broad-band electrostatic noise of the same type as that shown in Figures 2 and 3. No magnetic noise bursts comparable to those shown in Figures 2 and 3 are observed during this pass.

The fourth representative pass (Figure 5) is an outbound Imp 6 pass near local midnight at about 2330 magnetic local time (at $R = 4.9\ R_E$). The plasma wave phenomena occurring during this pass are even more complicated and difficult to analyze than the preceding example. Although essentially the same plasma wave phenomena (auroral kilometric radiation, continuum radiation, plasmaspheric hiss, auroral hiss, and broad-band electrostatic noise) occur during this pass, in some cases it is very difficult to distinguish the different types of emissions. However, several distinct regions with intense broad-band electrostatic noise can be easily identified, the first at about 0527 UT, followed by several broad regions from about 0558 to 0625 UT, and the last at about 0650 UT. The enhanced electric field intensities associated with these regions are very clear and distinct, particularly in the peak field strength measurements. Again the maximum electric field intensities occur at low frequencies, from about 36 to 120 Hz, although some bursts of noise can be detected at frequencies as high as 10 kHz. At high frequencies, particularly in the 5.62-kHz channel, the ratio of peak to average field strengths is quite large (~50 dB), indicating that at these frequencies the broad-band electrostatic noise is very impulsive, consisting of many brief but intense bursts. Magnetic noise bursts are also clearly evident in the same region in which the broad-band electrostatic noise occurs.

The four passes which have just been discussed are intended to illustrate the types of plasma waves observed by Hawkeye 1 and Imp 6 in the high-latitude region of the magnetosphere. It is evident in these passes and many other similar passes which have been examined that a distinct, easily identified region of low-frequency electric field turbulence is present on the high-latitude auroral field lines at essentially all local times. The main observational characteristics of this turbulence, which has been called broad-band electrostatic noise, are that (1) it is very intense, with electric field strengths up to 10 mV m^{-1} and occasionally larger, (2) it is most intense in the frequency range of about 10–50 Hz, and (3) it occurs over a relatively wide region, usually several degrees in magnetic latitude, at L values of typically 8–12. The detailed characteristics of this noise are described in the following sections.

Frequency Spectrums

A typical frequency spectrum of the broad-band electrostatic noise is shown in Figure 6. This spectrum was selected from the Hawkeye 1 pass in Figure 2 at about the time of peak intensity, from 1240 to 1243 UT. The two spectrums shown in Figure 6 give the peak and average electric field spectral densities from each frequency channel during this interval. The rms electric field strength obtained by integrating the average electric field spectral density over all frequencies is 10.8 mV m^{-1}, and the corresponding peak electric field strength is about 35.6 mV m^{-1}. The main contribution to the rms electric field strength comes from the frequency range of about 10–50 Hz. At high frequencies, above about 100 Hz, the electric field intensity decreases very rapidly with increasing frequency, and a moderately sharp cutoff is evident at about 10 kHz. This upper cutoff occurs near the local electron gyrofrequency f_g^-. At low frequencies, below about 10 Hz, the electric field intensity decreases with decreasing frequency, and a distinct maximum occurs in the frequency spectrum at about 20 Hz. As indicated in Figure 6, this maximum is in the frequency range between the local proton gyrofrequency f_g^+ and the hybrid frequency $(f_g^+ f_g^-)^{1/2}$. The exact shape of the spectrum at frequencies below about 10 Hz is somewhat uncertain because of the high levels of spacecraft-generated interference

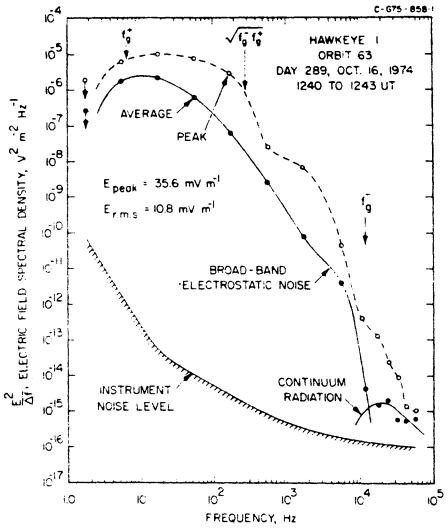

Fig. 6. An electric field spectrum of the broad-band electrostatic noise at about the time of maximum intensity for the pass shown in Figure 2. This event is typical of the most intense events of this type detected by either Hawkeye 1 or Imp 6.

(from the solar panels) at these low frequencies. Usually, the broad-band electrostatic noise is not detectable in the 1.78-Hz electric field channel, and the largest field strengths are detected in either the 17.8- or the 56.2-Hz channel.

To compare the electric field and magnetic field spectrums, the magnetic field spectrum for the same interval is shown in Figure 7. Again both peak and average spectrums are shown. The magnetic noise intensities are seen to be significantly above the instrument noise levels for all frequencies below about 1.0 kHz. Both the peak and the average magnetic field intensities show a distinct maximum in the spectrum at about 50 Hz. This maximum is associated with the magnetic noise bursts indicated in Figure 2. The rms and peak magnetic field strengths of this noise, integrated from 5.6 Hz to 1.78 kHz, are about 5.8 and 36.8 mγ, respectively. The large difference between the peak and average field strengths is caused by the large fluctuations in the field strengths which are clearly evident in Figure 2. The ratio of the average electric field energy density to the average magnetic field energy density in this case is $E^2/C^2B^2 \simeq 39$, which confirms the electrostatic (or at least quasi-electrostatic) character of the broad-band electrostatic noise detected in this region. Below about 10 Hz, a weak low-frequency component is evident slightly above the receiver noise level, increasing in intensity toward lower frequencies. This monotonic low-frequency component is probably associated with the magnetic field perturbations evident in the θ^B angle at about this time (see Figure 2). Whether this low-frequency component represents an ambient wave spectrum, as is almost certainly the case for the magnetic noise bursts detected at higher frequencies, or simply the spacecraft motion through spatial gradients in the magnetic field cannot be determined.

Further details regarding the frequency-time structure of these emissions can be obtained from the wide-band wave form data. High-resolution frequency-time spectrograms of the broad-band electrostatic noise and magnetic noise bursts observed during the Imp 6 pass in Figure 5 are shown in Figure 8. Two different frequency scales, 0–1 kHz and 0–200 Hz, are used to provide good frequency resolution over the entire frequency range. For the mode of operation being used during this pass the wave form receiver alternately switches between the electric and magnetic antennas once every 20.48 s. The electric field spectrums of the broad-band electrostatic noise in Figure 8 show remarkably little temporal structure. The rapid decrease in the intensity with increasing frequency is clearly evident. A few impulsive bursts can be seen extending to frequencies above 1 kHz. At low frequencies a distinct low-frequency cutoff is evident at a frequency which varies from about 20 to 50 Hz. Although this cutoff is near the low-frequency limit of the wave form receiver, the temporal variations show that this cutoff is not caused by instrumental effects. At certain times, for example, at about 0619:25 and 0620:10 UT, the noise becomes very intense near this cutoff and develops into a strong emission at about 50 Hz. Comparisons between successive electric and magnetic spectrograms show that the magnetic field spectrum is quite different from the electric field spectrum. Generally, the magnetic field intensities are very low, and it is very difficult to clearly identify the magnetic noise bursts evident in the magnetic field channels of Figure 5. The magnetic noise bursts usually comprise poorly defined emissions lasting only a few seconds at about 50–100 Hz, as evident, for example, at about 0619:50 and 0620:34 UT in Figure 8. Occasionally, as at about 0620:36 UT, a diffuse burst with a rapidly varying center frequency can be seen extending to frequencies above 1 kHz. In some cases it appears that the strong electric field enhancements near the lower cutoff frequency of the broad-band electrostatic noise may be directly associated with the quasi-monochromatic magnetic noise bursts. Unfortunately, we do not have suitable simultaneous electric and magnetic field spectrograms to definitely establish this relationship.

REGION OF OCCURRENCE

The examples of broad-band electrostatic noise which have been shown have all been at L values typical of the auroral field lines. We would now like to definitely establish the region of occurrence of this noise, using the extensive measurements obtained by Hawkeye 1 and Imp 6. Since an extremely large number of measurements are to be surveyed (14 months of data from Hawkeye 1 and 3.5 years of data from Imp 6), a simple criterion must be used to provide automatic computer identification of the broad-band electrostatic noise. As has

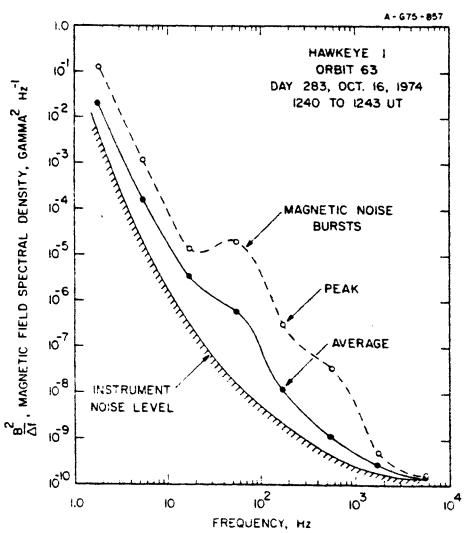

Fig. 7. A magnetic field spectrum of the magnetic noise bursts detected during the same interval as the spectrum in Figure 6.

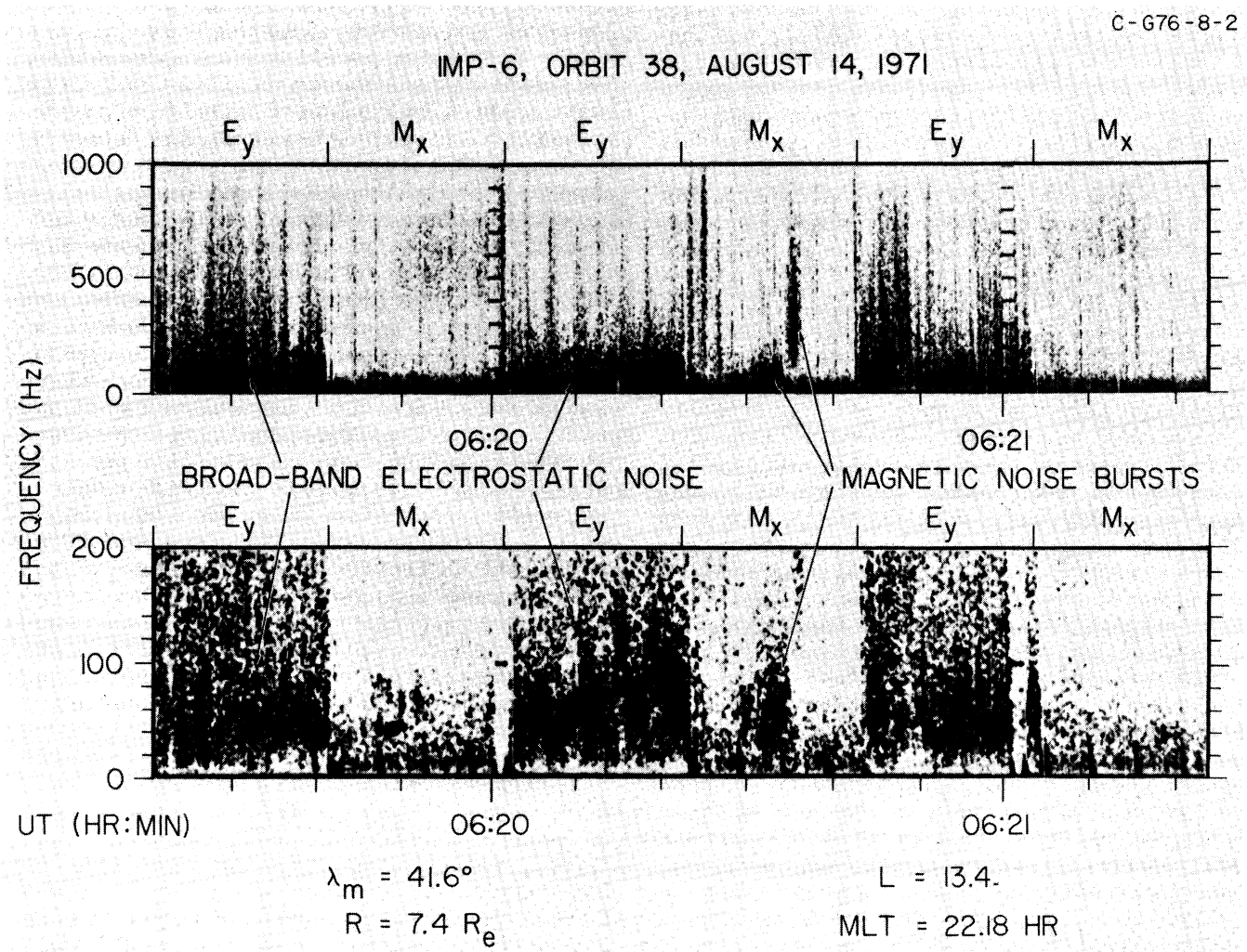

Fig. 8. Wide-band frequency-time spectrums of the electric (E_y) and magnetic (M_y) fields detected by Imp 6 during a period of enhanced broad-band electrostatic intensity during the pass shown in Figure 5. The spectrum of the broad-band electrostatic noise shows little structure at low frequencies except for a distinct low-frequency cutoff at about 20–50 Hz. The magnetic noise bursts are also very diffuse and difficult to identify.

been previously discussed, the broad-band electrostatic noise is usually most intense in the frequency range of about 10–50 Hz. Fortunately, except for the earth's bow shock, no other type of magnetospheric plasma wave emission has electric field intensities comparable to the broad-band electrostatic noise in this frequency range. The broad-band electrostatic noise can therefore be identified with good reliability on the basis of the low-frequency electric field intensities. For this study we have chosen to use the peak electric field intensities in the 56.2-Hz channel of Hawkeye 1 and in the 63.0-Hz channel of Imp 6 for identifying these events. Several electric field thresholds have been tried, and a threshold electric field spectral density of 1.4×10^{-7} V^2 m^{-2} Hz^{-1} has been selected. This threshold represents a reasonable compromise between obtaining too few events if the threshold is set too high and obtaining too many false identifications from other plasma wave phenomena if the threshold is set too low.

Figures 9 and 10 show the magnetic meridian plane (R, λ_m) coordinates of all of the events in the 14 months of Hawkeye 1 data and 3.5 years of Imp 6 data which exceed the selected threshold. Figure 9 shows the events which occurred in magnetic local time quadrants centered on local noon (0900–1500 MLT) and local midnight (2100–0300 MLT), and Figure 10 shows the corresponding data for local dawn (0300–0900 MLT) and local dusk (1500–2100 MLT). Each point represents a specific interval, 184.3 s for Hawkeye 1 and 327.6 s for Imp 6, during which the electric field intensity exceeded the selected threshold. The approximate outline of the combined region sampled by the two spacecraft is indicated by the dashed lines in each quadrant. Although these plots do not provide a precise indication of the frequency of occurrence because of the difference in the number of data from each satellite and the complexity of the orbital coverage, they do provide a good qualitative picture of where the broad-band electrostatic noise is observed. Almost without exception the noise is observed on magnetic field lines which connect with the high-latitude auroral regions. The noise is observed over a large range of radial distances, from about 1.5 R_E to greater than 15 R_E. Although most of the events are observed at radial distances greater than about 4 R_E, this boundary is seen to be

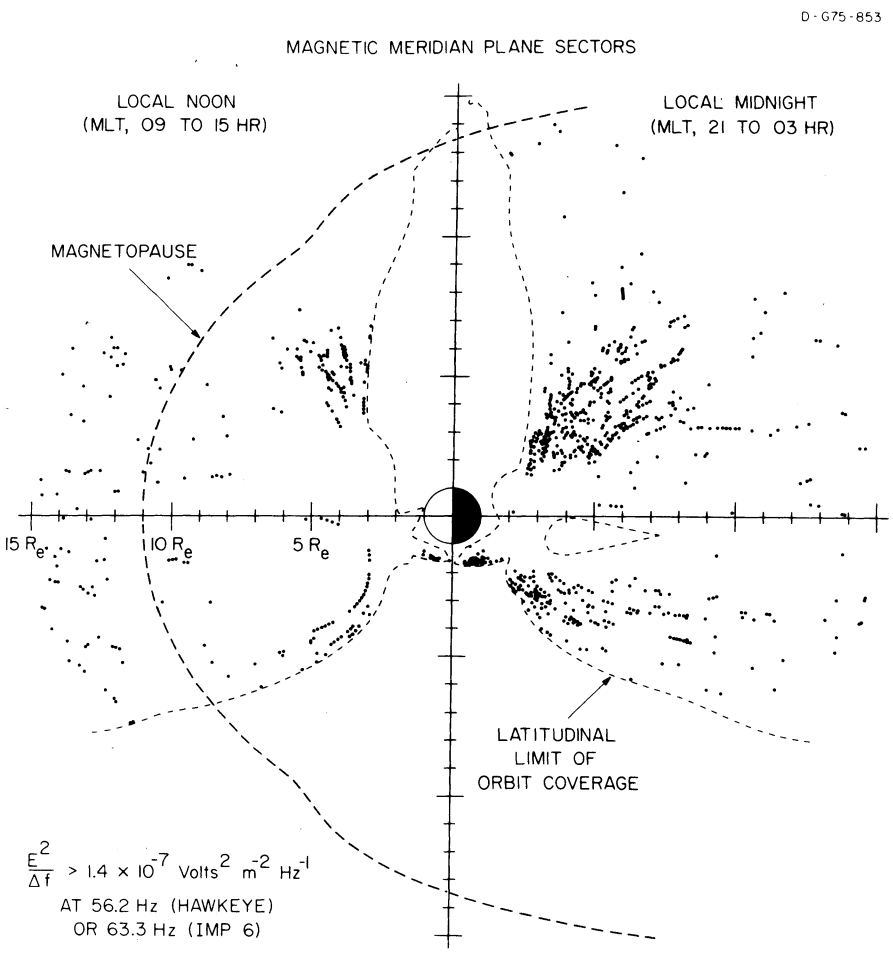

Fig. 9. Magnetic meridional plane (R, λ_m) plots for magnetic local times (MLT) near local noon and local midnight of all the Hawkeye 1 and Imp 6 electric field intensities which exceed a preset threshold. The threshold intensity and frequencies are chosen to provide reasonably reliable identification of intense broad-band electrostatic noise events. A few of the events beyond about 10 R_E in the local noon sector are caused by electrostatic noise associated with the bow shock and magnetosheath. Most of the events occur at high magnetic latitudes at L values typical of the auroral field lines.

primarily a limitation imposed by the orbital coverage, since essentially no measurements are obtained on auroral field lines at radial distances between about 1.8 and 4.0 R_E. A very dense concentration of points can be seen over the southern auroral region at radial distances from about 1.5 to 1.8 R_E. These data also show that the broad-band electrostatic noise is observed at all local times, although relatively few events are evident in the local noon quadrant. The widely scattered events evident beyond about 10 R_E in the local noon quadrant are caused by electrostatic noise associated with the bow shock and magnetosheath and not by broad-band electrostatic noise.

To take into account the effects of the orbital coverage, we have performed a detailed analysis of the frequency of occurrence of the events shown in Figures 9 and 10. For this analysis the R, λ_m and MLT coordinate system has been divided into boxes, and the number of events counted once per orbit and the number of orbits passing through each box are determined. The frequency of occurrence is given by the ratio of the number of events to the number of orbits counted in each box. The essential features of the frequency of occurrence distribution determined from this analysis are summarized in Figures 11 and 12. Figure 11 shows the frequency of occurrence as a function of radial distance and magnetic latitude for magnetic local times in the local midnight quadrant, from about 2100 to 0300 MLT. These data clearly show that the broad-band electrostatic noise occurs in two distinct latitudinally symmetric regions, starting at high latitudes, ~70°, near the earth and extending to progressively lower latitudes with increasing radial distance. The two regions appear to merge in the magnetotail at a radial distance of about 10 R_E. The latitudinal width of the region of occurrence, approximately 20° at R = 4.01 and 6.31 R_E, is several times larger than the latitudinal width typically observed on an individual pass. This increase in the apparent latitudinal width of the region of occurrence is almost certainly caused by the orbit-to-orbit variations of the L shell on which the noise occurs. The regions of occurrence shown in these illustrations must not be viewed as an instantaneous picture of the region in which the noise occurs. At large distances from the earth, $R \gtrsim 10\ R_E$, the ability of the magnetic field model (for λ_m and MLT) to represent the real field is also subject to large errors. The tendency of the latitudinal width of the region of occurrence to increase with increasing radial distance is probably due in part to errors of this type. For the threshold used in this analysis the maximum frequency of occurrence is about 20%. Because of temporal variations of the L shell on which the noise is detected a more meaningful parameter is probably the percentage occurrence of the broad-band electrostatic noise during a given pass across the auroral L shells. For the threshold used in Figures 11 and 12 this percentage occurrence is about 50–60% in the region near local midnight. The absolute frequency of occurrence should not be considered of fundamental importance,

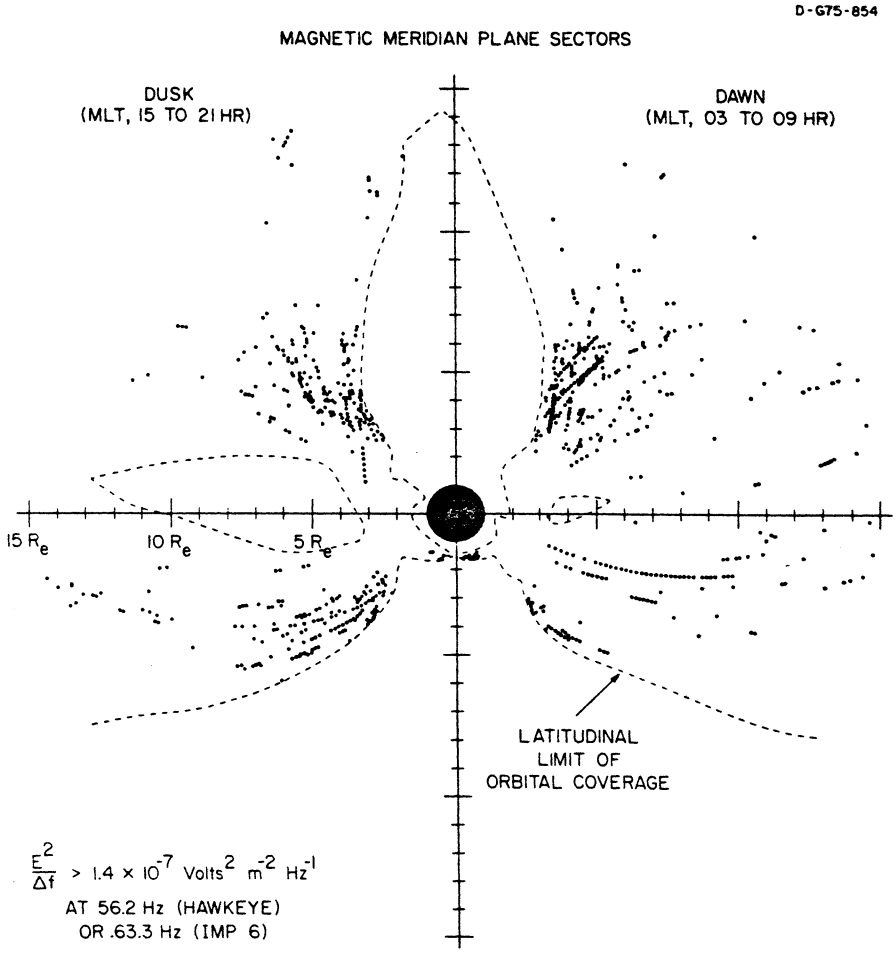

Fig. 10. Magnetic meridian plane plots comparable to Figure 9 for magnetic local times near local dawn and dusk.

since it depends somewhat on the choice of the threshold field strength. However, the region of occurrence on auroral field lines extending back into the distant magnetotail is relatively insensitive to this threshold.

To illustrate the variations in the region of occurrence with magnetic local time, Figure 12 shows the frequency of occurrence as a function of magnetic latitude and magnetic local time at a constant radial distance, $5.01\ R_E \leq R < 6.31\ R_E$. This range of radial distances was chosen because it is sufficiently far from the earth to provide measurements over a wide range of magnetic latitudes and still close enough for the magnetic field model to be reasonably accurate. For reference, the L value of the magnetic field passing through $R = 5.62\ R_E$ is shown on the right side of Figure 12. The broad-band electrostatic noise is seen to occur in an essentially continuous band at all local times around the earth. The noise occurs at the lowest magnetic latitudes near local midnight and at systematically higher magnetic latitudes on the dayside of the earth. Near local midnight the maximum occurrence is at L values from about 8 to 12.

Relationship to Auroral Hiss

Observations

Auroral hiss is a broad-band whistler mode emission commonly observed in the auroral regions by low-altitude polar-orbiting satellites. As is indicated in Figures 4 and 5, auroral hiss has also been observed at high altitudes in the magnetosphere by Hawkeye 1 and Imp 6. Although the broad-band electrostatic noise sometimes occurs in regions where no auroral hiss can be identified, as in Figures 2 and 3, in some cases these two types of noise occur in the same region of the magnetosphere and appear to be closely related. This relationship is illustrated by the two Hawkeye 1 passes in Figures 13 and 14. Both of these passes occur near local midnight, and the plasma wave phenomena observed are qualitatively similar to Figures 4 and 5. In both cases the auroral hiss emissions are easily identified in the wide-band spectrograms by the characteristic broad-band noise spectrum, with little temporal structure, extending from a few hundred hertz to several kilohertz. A distinct upper cutoff frequency is evident at a frequency slightly below the local electron gyrofrequency (indicated by the dashed lines marked f_g^-). This cutoff occurs because the whistler mode cannot propagate at frequencies above the electron gyrofrequency. The spectrogram in Figure 13 also clearly shows the distinct gap between the auroral hiss and continuum emissions which is usually not apparent in the coarse frequency resolution measurements (as in Figure 4). The auroral hiss spectrum from about 1100 to 1230 UT in Figure 14, and to some extent in Figure 13, has a distinct V-shaped lower-frequency cutoff which bears an unmistakable similarity to the V-shaped low-frequency cutoff of the auroral hiss observed by low-altitude satellites [see *Gurnett*, 1966; *Gurnett and Frank*, 1972*a*].

In the top panel of Figure 13, several periods of enhanced electric field intensity, characteristic of the broad-band electrostatic noise, can be seen from about 1207 to 1300 UT, between the two regions where the auroral hiss is observed. In

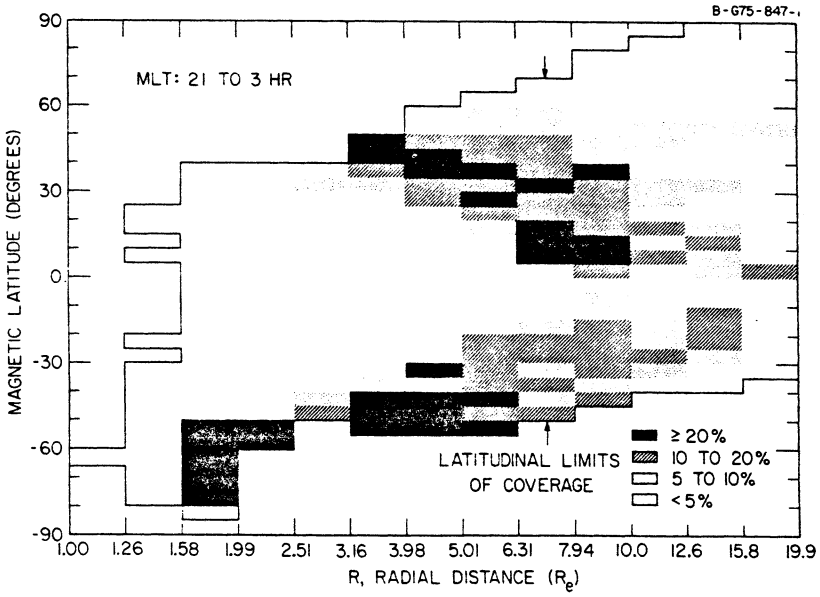

Fig. 11. The normalized frequency of occurrence of the broad-band electrostatic noise as a function of magnetic latitude and radial distance in the 2100–0300 magnetic local time sector near local midnight. The electric field threshold is the same as in Figures 9 and 10.

the wide-band spectrograms the broad-band electrostatic noise appears as a distinct increase in the intensity near the low-frequency limit of the spectrogram. Note that the wide-band spectrograms (which are obtained by using an automatic gain control receiver) show only the relative intensity at different frequencies, whereas the fixed frequency channels give the absolute intensity. Thus even though the wide-band spectrograms indicate that the auroral hiss has completely disappeared in the region where the broad-band electrostatic noise is observed, the fixed frequency channels (1.78 kHz, in particular) show that the auroral hiss intensity actually increases slightly in this region. The broad-band electrostatic noise therefore can be interpreted as a lowering and intensification of the low-frequency portion of the auroral hiss spectrum. This transition from the auroral hiss to the broad-band electrostatic noise is shown even more clearly by the example in Figure 14. In this case the enhanced electric field intensities in the 56.2-Hz electric field channel place the region of broad-band electrostatic noise from about 1135 to 1200 UT. Inspection of the wide-band spectrograms shows that this noise is essentially indistinguishable from the auroral hiss.

Discussion

Because of the close relationship between the auroral hiss and the broad-band electrostatic noise the question arises whether there is any essential difference between these two types of noise. The auroral hiss detected by Hawkeye 1 and Imp 6 is clearly a whistler mode electromagnetic emission which propagates a considerable distance through the magnetosphere. The simultaneous detection of both the electric and

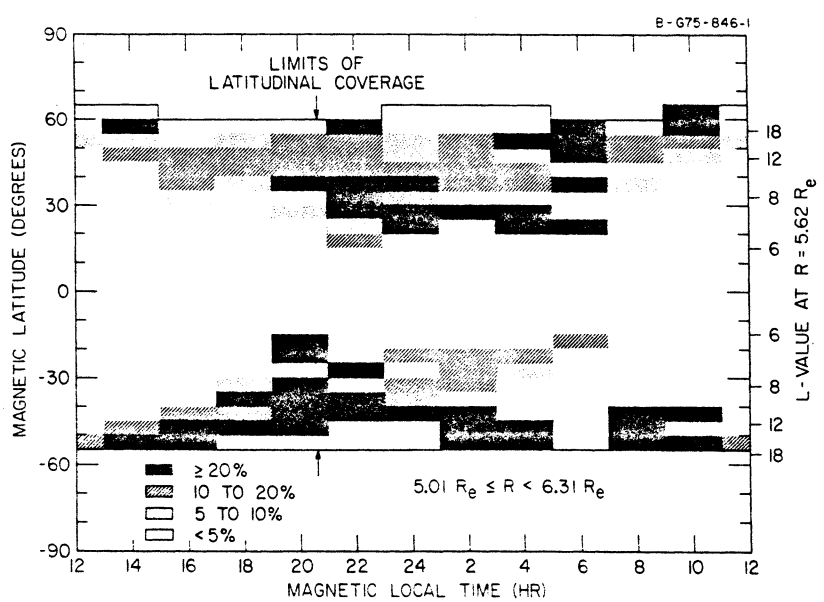

Fig. 12. The normalized frequency of occurrence of the broad-band electrostatic noise as a function of magnetic latitude and magnetic local time within the radial-distance range 5.01–6.31 R_E. The L value of the magnetic field line which intersects $R = 5.62\ R_E$ is shown on the right for comparison with low-altitude measurements.

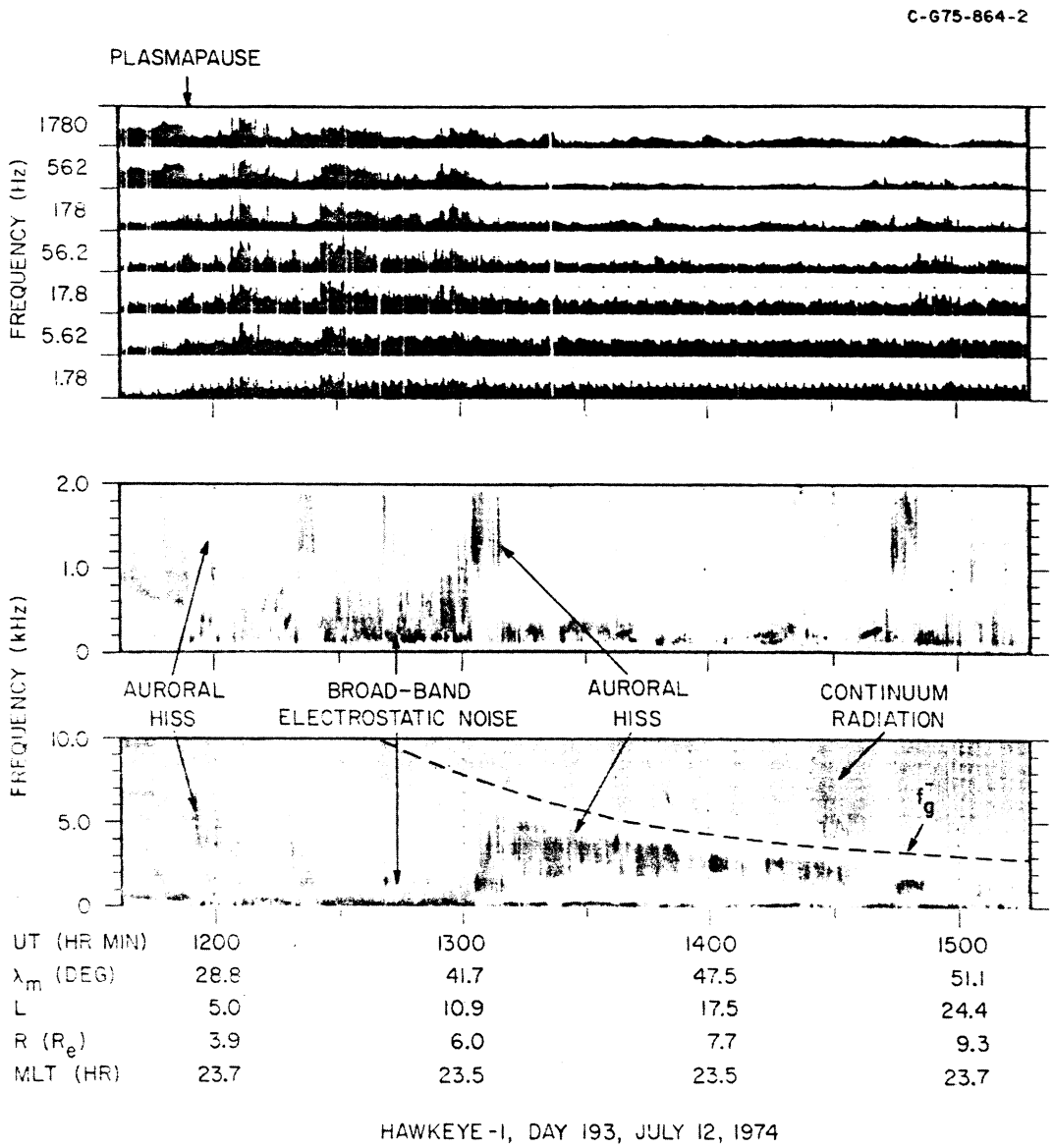

Fig. 13. Frequency-time spectrograms showing the relationship between auroral hiss and broad-band electrostatic noise during an outbound Hawkeye 1 pass near local midnight. The broad-band electrostatic noise sometimes appears as a lowering and intensification of the low-frequency cutoff of the auroral hiss spectrum. The distinct cutoff of the auroral hiss at a frequency slightly below the local electron gyrofrequency f_g^- and the gap between the auroral hiss ($f < f_g^-$) and continuum radiation ($f > f_p^-$) are clearly evident.

the magnetic field of the auroral hiss, as in Figure 4, shows that the emission is an electromagnetic wave, and the frequency range $f < f_g^-$ unmistakably identifies the mode of propagation as the whistler mode. The V-shaped low-frequency cutoff of the auroral hiss can be explained from simple ray path considerations if the noise is generated along an auroral field line below the spacecraft, as shown in Figure 15. It is a well-known characteristic of the whistler mode that the ray paths are guided somewhat along the magnetic field line and that this guiding effect is frequency dependent. If the emission is generated at wave normal directions near the resonance cone, as is thought to be the case for auroral hiss observed at low altitudes [*Taylor and Shawhan*, 1974], then the angle that the ray path makes with respect to the magnetic field increases with increasing frequency, varying from 0° at the lower hybrid resonance frequency f_{LHR} to 90° at the electron gyrofrequency. This frequency dependence causes the ray paths to deviate increasingly from the magnetic field line as the wave frequency approaches the electron gyrofrequency. The effect of this frequency dependence is to allow the emission to be observed over a larger spatial region at higher frequencies (compare f_1 and f_2 in Figure 15), thus producing the V-shaped low-frequency cutoff.

In contrast to the electromagnetic auroral hiss, which propagates large distances from the L shell on which it was generated, the broad-band electrostatic noise is observed in a very localized region and has no detectable magnetic field component, as would be expected for a local electrostatic plasma instability. Despite these marked differences the wide-band spectrums, as in Figure 14, sometimes show a nearly continuous transition between the auroral hiss and the broad-band electrostatic noise. These observations strongly suggest that the electrostatic noise is closely related to the generation of the auroral hiss. *Taylor and Shawhan* [1974] have shown that for

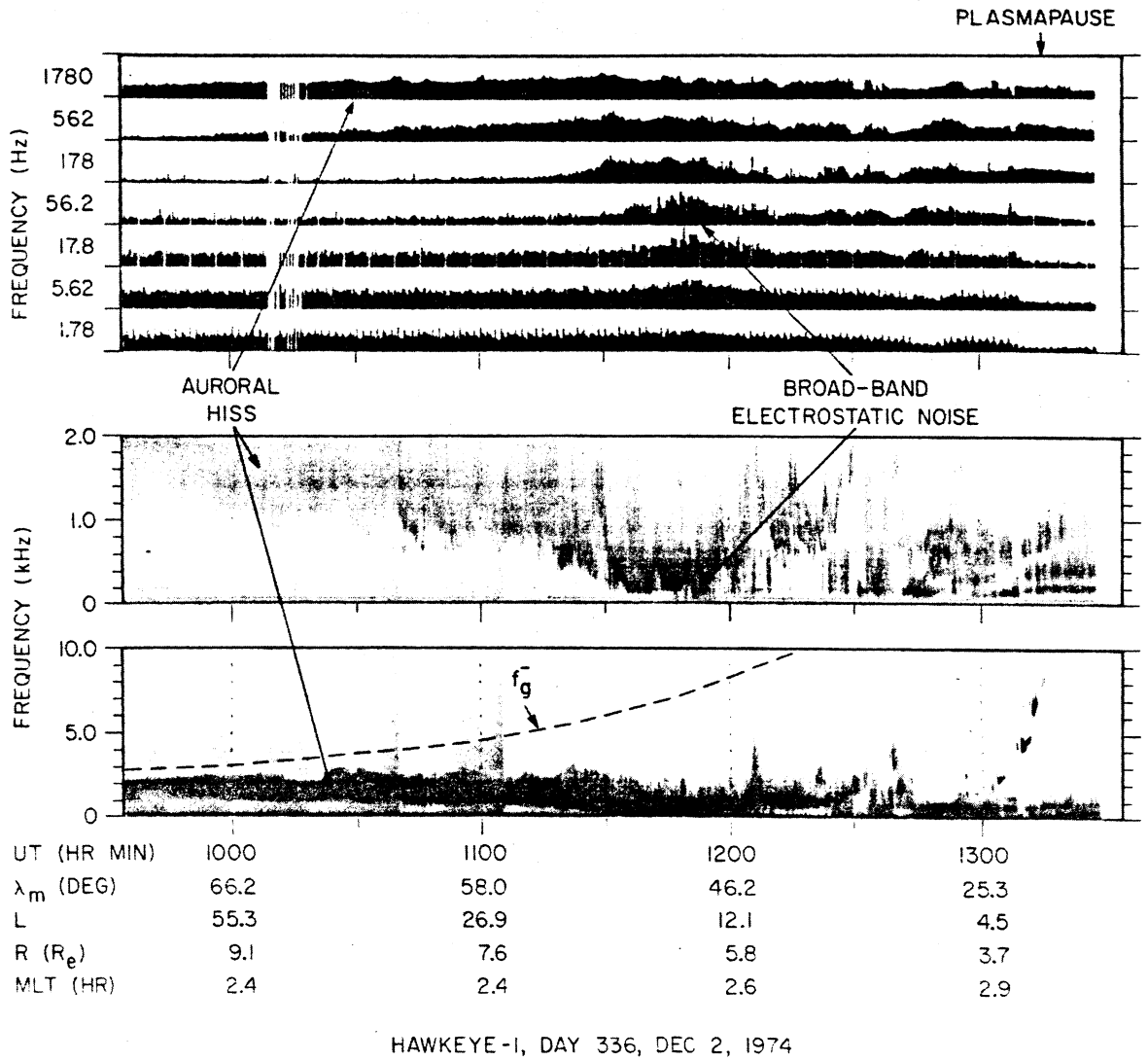

Fig. 14. Another case, similar to Figure 13, showing auroral hiss and broad-band electrostatic noise during an inbound Hawkeye 1 pass in the early morning. In this case, no clear distinction can be made between the auroral hiss and the broad-band electrostatic noise.

wave normal directions very close to the resonance cone the whistler mode takes on characteristics of a local electrostatic wave, with short wavelengths, small magnetic field components, and low phase velocities. If the broad-band electrostatic noise is closely coupled to these short-wavelength whistler mode waves or represents an extension of the same plasma wave mode, it seems entirely possible that the auroral hiss is generated directly from this electrostatic noise by changes in the wave normal direction at plasma boundaries and density irregularities. Processes of this type have already been suggested by *Maggs* [1976] for generation of auroral hiss.

Relationship to Magnetospheric Plasmas and Field-Aligned Currents

Observations

We now consider the relationship of the intense electric field turbulence detected by Hawkeye 1 and Imp 6 to the plasmas and field-aligned currents which are present in the high-latitude auroral regions of the magnetosphere. To illustrate the plasma relationships which are typically observed, Plate 1 shows the charged particle intensities for the inbound Hawkeye 1 pass in Figure 2 during the period in which the intense broad-band electrostatic noise is detected. The top two panels of Plate 1 show the energy-time spectrograms of electron and proton intensities detected by the Lepedea, and the bottom panel gives the counting rate ($\log_{10}$) of the thin-windowed GM tube. The Lepedea on board Hawkeye 1 provides measurements of the differential energy spectrums of protons and electrons within the energy range 50 eV $\leq E \leq$ 40 keV, and the GM tube responds to electrons with energies $E >$ 45 keV and protons with energies $E >$ 650 keV. In comparing Figure 2 and Plate 1 it is evident that the region of intense broad-band electrostatic noise observed during this pass, with maximum intensities from about 1234 to 1244 UT, occurs just before the rapid increase in the GM tube counting rate and in a region

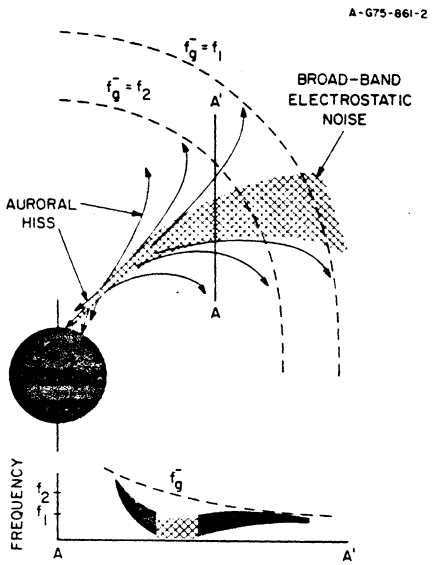

Fig. 15. A qualitative model showing the region of broad-band electrostatic noise and the ray paths of the auroral hiss suggested by events such as in Figure 14. The ray paths of the whistler mode auroral hiss tend to deviate from the local magnetic field direction as the wave frequency approaches the electron gyrofrequency. The frequency dependence of the ray path can account for the V-shaped low-frequency cutoff.

with substantial fluxes of low-energy (~1 keV) protons. The rapid increase in the GM tube counting rate at about 1242 UT, which is shown in more detail in Figure 16, marks the entrance into the stably trapped region of the outer radiation zone and is a characteristic boundary called the electron $E > 45$ keV trapping boundary. Low-altitude measurements of convection electric fields show that the $E > 45$ keV trapping boundary usually corresponds closely with the boundary between open and closed magnetic field lines [*Frank and Gurnett*, 1971; *Gurnett and Frank*, 1973]. The low-energy electron and proton spectrums in the region in which the broad-band electrostatic noise is observed are characteristic of the high-density plasma typically found in the magnetosheath and polar cusp. The relationship of the electrostatic noise to the $E > 45$ keV trapping boundary and to the low-energy plasma in this case is qualitatively similar to events of the type previously discussed by *Scarf et al.* [1973, 1975]. After crossing the trapping boundary a region of very intense (1–10 keV) electron intensities is encountered from about 1245 to 1310 UT. These more energetic and intense electron fluxes are characteristic of the outer radiation zone during magnetically disturbed periods (a magnetic storm occurred 2 days earlier, on October 14, 1974).

Examination of charged particle measurements similar to those in Plate 1 and Figure 16 for other local times shows that the region of broad-band electrostatic noise is consistently observed near and always on the poleward side of the electron $E > 45$ keV trapping boundary, outside the energetic (1–10 keV) electron intensities characteristic of the plasma sheet and outer radiation zone. The region of intense electric field turbulence is usually characterized by a distinct increase in the low-energy (100 eV to 1 keV) electron and proton intensities. Several types of measurements show that a distinctly different higher-density plasma is encountered in this region. In Figure 3 a sharp cutoff is evident in the continuum radiation (in the 13.3-kHz channel, in particular) at about the time, ~1825 UT, that the broad-band electrostatic noise is encountered. The cutoff is almost certainly caused by an abrupt increase in the plasma frequency and hence plasma density in the region where the broad-band electrostatic noise is observed. This increase in the plasma density is directly confirmed by the Lepedea data for this pass illustrated in Plate 2, which shows an abrupt increase in the low-energy (100 eV to 1 keV) electron and proton intensities characteristic of magnetosheath and polar cusp plasma at about 1825 UT. The static electric field measurement on Hawkeye 1, which is very sensitive to changes in the plasma density and temperature, also usually indicates an abrupt discontinuity at the boundaries of the region where the broad-band electrostatic noise is observed.

The Hawkeye 1 magnetic field data have been carefully examined in search of magnetic field perturbations caused by field-aligned currents in the region where the broad-band electrostatic noise is observed. In most cases, no corresponding magnetic field perturbations can be detected. However, in a few cases, magnetic field perturbations occur which are almost certainly associated with field-aligned currents. One of these cases is illustrated in Figure 2. The magnetic field measurements in Figure 2 clearly show numerous small perturbations in the angle θ^B as the spacecraft passes through the region in which the most intense broad-band electrostatic noise is detected. These magnetic field perturbations have not yet been analyzed in detail because of the previously mentioned problem of reconstructing the spacecraft attitude during the periods in question. However, the magnetic field signature given by the angle θ^B, when compared with similar measurements of this type by *Aubry et al.* [1972] and *Fairfield* [1973], provides convincing evidence that field-aligned currents are present in the region where the broad-band electrostatic noise occurs. Similar magnetic field perturbations indicative of field-aligned currents are also evident in Figure 5 and to a lesser extent in Figure 4. The magnetic field measurements in Figure 3 show a somewhat different magnetic field signature which has been observed several times on the dayside of the earth. In this case a marked change in the slope of θ^B versus time is evident as the spacecraft enters the region of broad-band electrostatic noise at about 1825 UT. As the spacecraft passes through the region of most intense electrostatic noise, from 1830 to 1930 UT, θ^B

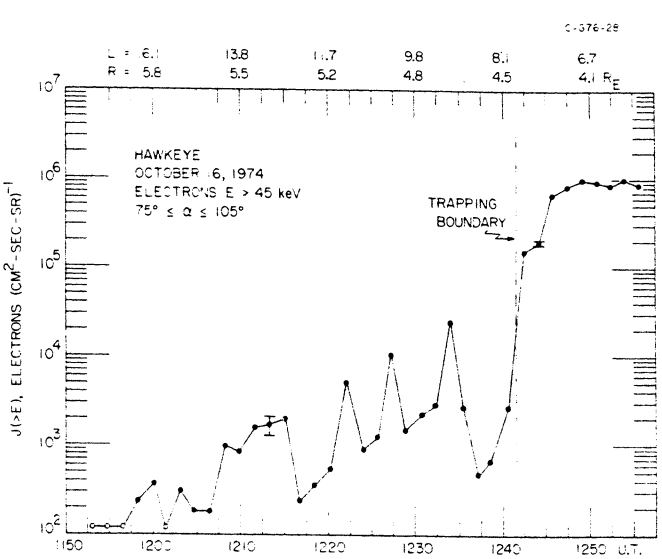

Fig. 16. The electron intensities with $E > 45$ keV, which were obtained with the GM tube for the pass shown in Plate 1. The electron $E > 45$ keV trapping boundary is located at about 1242 UT. This boundary marks the entrance into the stably trapped region of the outer radiation zone.

changes by about 45°, and many small amplitude fluctuations are evident in both the magnitude and the direction of the field. Both the skewing of the magnetic field direction and the small-scale fluctuations indicate that the spacecraft has entered a region of higher β (ratio of the plasma to magnetic field pressure) in which the plasma is producing significant local changes in the magnetic field. The abrupt increase in the low-energy (100 eV to 1 keV) proton intensities, shown in Plate 2, provides further evidence of the higher β in this region. The magnetic field in this region still remains sufficiently well ordered to rule out the possibility that the boundary at 1825 UT could be the magnetopause.

Discussion

It is evident that the broad-band electrostatic noise detected by Hawkeye 1 and Imp 6 corresponds to a distinct plasma region which extends along the magnetic field from low altitudes in the auroral zone into the distant magnetosphere. When these data are compared with low-altitude measurements in the local afternoon and evening, all of the available evidence indicates that the broad-band electrostatic noise occurs on magnetic field lines which connect with the region of intense inverted V electron precipitation observed by low-altitude polar-orbiting satellites [*Frank and Ackerson*, 1971]. This conclusion is supported by the following specific comparisons. (1) As was discussed in the previous section, the V-shaped auroral hiss events detected by Hawkeye 1 and Imp 6 appear to originate from the region in which the broad-band electrostatic noise is detected. At low altitudes, comparable V-shaped auroral hiss events are directly associated with inverted V events [*Gurnett and Frank*, 1972*a*] and can be reliably used to identify the inverted V electron precipitation region. (2) The low-frequency magnetic noise bursts detected by Hawkeye 1 and Imp 6, which occur in the same region as the broad-band electrostatic noise, appear to be the same as the whistler mode ELF noise bands reported by *Gurnett and Frank* [1972*b*] at low altitudes. These ELF noise bands also occur in the same region as the inverted V events and can be used as a good indicator of the inverted V electron precipitation region. (3) The broad-band electrostatic noise occurs in a region which is poleward of the electron $E > 45$ keV trapping boundary. At low altitudes the inverted V events have essentially the same relationship to the electron $E > 45$ keV trapping boundary [*Frank and Ackerson*, 1971]. (4) The broad-band electrostatic noise occurs in regions with substantial field-aligned currents. At low altitudes the inverted V events are also known to occur in regions with substantial field-aligned currents [*Ackerson and Frank*, 1972].

In the local morning the association of the broad-band electrostatic noise with the low-altitude inverted V electron precipitation is not as clearly established as in the local afternoon and evening. The location of the broad-band electrostatic noise, always immediately poleward of the $E > 45$ keV trapping boundary, suggests that the spatial relationship with the inverted V events is essentially the same in the local morning as in the local afternoon and evening. Unfortunately, in the local morning, most of the remaining methods of comparison either are absent or have not yet been adequately studied. For example, auroral hiss events with a distinct V-shaped low-frequency cutoff, which provide a method of identifying the inverted V region in the local afternoon and evening, are not observed in either the low-altitude or the high-altitude plasma wave measurements in the local morning. ELF noise bands, which also provide a method of identifying the inverted V region, have not been studied sufficiently in the local morning region at low altitudes to provide a basis for comparison.

When the Hawkeye 1 and Imp 6 measurements are compared with other measurements in the distant magnetosphere, a very clear relationship is found with plasma waves detected in the distant magnetotail. Recently, *Gurnett et al.* [1976], using data from the Imp 8 spacecraft at geocentric radial distances from about 23.1 to 46.3 R_E, reported observations of broad-band electrostatic noise and magnetic noise bursts with characteristics essentially identical to the noise detected by Hawkeye 1 and Imp 6 much closer to the earth. Actually, Imp 6 also detects this noise in the distant magnetotail (see Figure 11); however, only the near-earth results, $R \lesssim 10\ R_E$, are emphasized in this paper. In the distant magnetotail the broad-band electrostatic noise and magnetic noise bursts are detected by Imp 8 near the outer boundary of the plasma sheet in regions which have very large plasma streaming velocities, $>10^3$ km s^{-1}, directed either toward or away from the earth. The electrostatic noise intensities are often greatly enhanced during periods of intense auroral activity. On the basis of these and other comparisons, *Gurnett et al.* [1976] suggested that the broad-band electrostatic noise and magnetic noise bursts occur in regions of field-aligned currents which develop at the outer boundaries of the plasma sheet during periods of increased auroral activity [*Aubry et al.*, 1972; *Fairfield*, 1973]. The very close similarity between the broad-band electrostatic noise and magnetic noise bursts detected by Hawkeye 1 and Imp 6 near the earth and by Imp 8 in the distant magnetotail provides strong evidence that this noise is associated with field-aligned currents which map into the inverted V electron precipitation regions observed at low altitudes. The relationships between the plasma waves, plasma regions, and field-aligned currents suggested by these data on the nightside of the earth are summarized in Figure 17.

At other local times the relationships between the broad-band electrostatic noise and the plasma regions of the distant magnetosphere are not as well understood. On the dayside of the earth the distinct skewing of the magnetic field direction in the region where the broad-band electrostatic noise is detected, as in Figure 3, strongly suggests that this region corresponds to the 'entry layer' discussed by *Paschmann et al.* [1976]. Since the investigation of the polar cusp region with Hawkeye 1 is still in a preliminary stage, further study is needed to establish the relationship of the broad-band electrostatic noise to the plasma regions observed on the dayside of the earth.

SUMMARY AND INTERPRETATION

In this study we have shown that a region of intense plasma wave turbulence occurs on high-latitude auroral field lines at altitudes ranging from a few thousand kilometers in the ionosphere to greater than 40 R_E in the distant magnetotail. Two distinctly different components are evident in the spectrum of this turbulence, (1) an intense quasi-electrostatic component called broad-band electrostatic noise and (2) a weak whistler mode electromagnetic component called magnetic noise bursts. The broad-band electrostatic noise occurs over a very broad frequency range, a few hertz to several kilohertz, with maximum electric field intensities in the frequency range of about 10–50 Hz and typical maximum broad-band rms electric field strengths of 10 mV m^{-1}. The magnetic noise bursts occur in the frequency range of about 10 Hz to a few hundred hertz (always with $f < f_g^-$) and are usually most intense at frequencies of about 100 Hz, with typical broad-band magnetic field

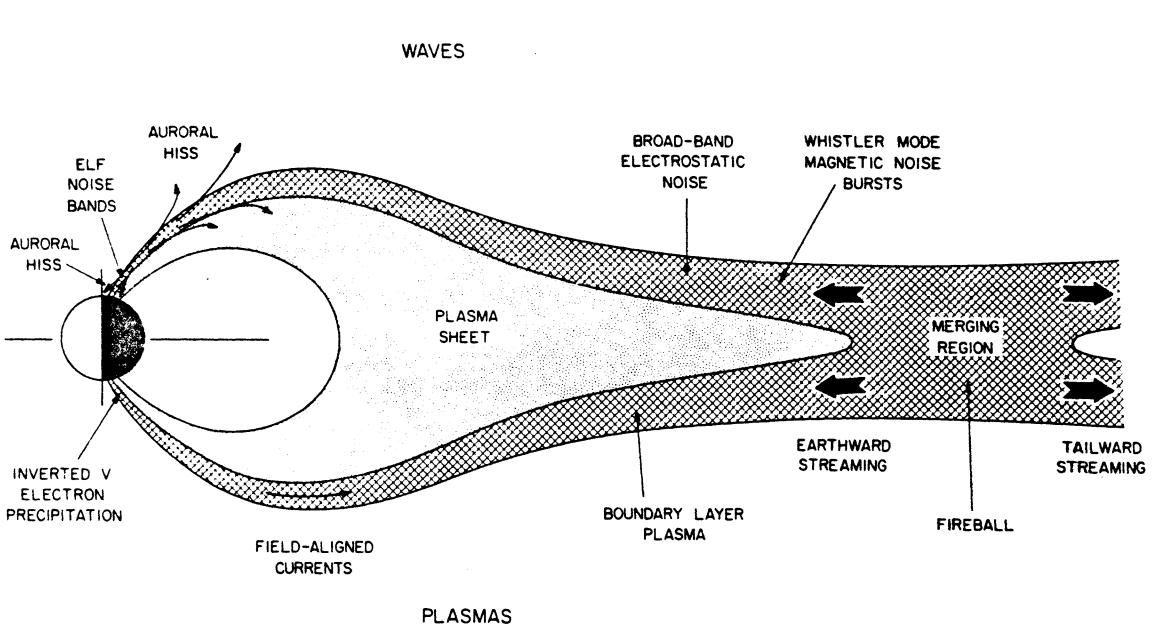

Fig. 17. The spatial relationships between the broad-band electrostatic noise, field-aligned currents, low-altitude inverted V electron precipitation, and earthward streaming protons in the distant magnetotail suggested by this study.

strengths of about 10 mγ. The magnetic noise bursts are always observed in the same region as the broad-band electrostatic noise. In the local afternoon and evening the broad-band electrostatic noise appears to have a close relationship with auroral hiss emissions which occur in this local time region. Comparison with low-altitude measurements provides substantial evidence that the intense plasma wave turbulence detected by Hawkeye 1 and Imp 6 occurs on magnetic field lines which connect with regions of intense inverted V electron precipitation observed at low altitudes. In the distant magnetotail the same plasma wave turbulence is detected by the Imp 8 spacecraft in regions with intense fluxes of protons streaming toward the earth at velocities sometimes in excess of 10^3 km s^{-1}. At intermediate radial distances, magnetic field perturbations characteristic of field-aligned currents have been detected in the same region as the intense plasma wave turbulence.

When these results are compared with other previous electric field measurements, it is apparent that the broad-band electric field turbulence detected by Hawkeye 1 and Imp 6 has many close similarities to the electric field turbulence detected by the Ogo 5 spacecraft in the high-latitude regions of the magnetosphere [*Scarf et al.*, 1973, 1975]. In both cases, intense electric field turbulence is observed near the energetic ($E \gtrsim 50$ keV) electron trapping boundary and in regions with large field-aligned currents. However, substantial differences are also evident. The most intense component of the broad-band electric field turbulence detected by Hawkeye 1 and Imp 6 occurs at frequencies (10–50 Hz) which are well below the low-frequency cutoff (~500 Hz) of the Ogo 5 plasma wave experiment and therefore not detectable. Within the frequency range of the Ogo 5 experiment the electrostatic turbulence usually consists of a few very impulsive bursts with durations of only a few seconds. In contrast, the low-frequency component of the electrostatic noise detected by Hawkeye 1 and Imp 6 occurs over a broad region, usually several degrees in magnetic latitude, with a nearly constant intensity. Frequently, short duration bursts can be seen in the Hawkeye 1 and Imp 6 wide-band spectrograms, as in Figure 8, extending upward in frequency out of the intense low-frequency component. These brief bursts probably correspond to the intense short duration bursts detected by Ogo 5.

Although most of the general features of this plasma wave turbulence are now known, many questions remain concerning the plasma wave modes involved in this turbulence and the role which these waves play in the plasma processes which occur along the auroral field lines. Although the mode of propagation of the magnetic noise bursts can be clearly identified as the whistler mode, the plasma wave mode associated with the broad-band electrostatic noise is poorly understood. The nearly continuous transition of the whistler mode auroral hiss spectrum into the broad-band electrostatic noise (as in Figures 13 and 14) suggests that the broad-band electrostatic noise is closely associated with the whistler mode. As was discussed earlier, very short wavelength whistler mode waves, with wave normal directions close to the resonance cone, have many of the characteristics required to explain this noise (they are quasi-electrostatic, have a low-frequency cutoff near f_{LHR}, and have small phase velocities characteristic of a spatially localized plasma wave mode). Although the broad-band electrostatic noise has certain characteristics of the cold plasma whistler mode, hot plasma effects must certainly be involved in the generation of this noise. Most likely, this noise is associated with a hot plasma mode, such as the ion sound wave mode ($f < f_{p^+}$) or the electrostatic ion cyclotron modes ($f \simeq nf_{g^+}$), which couple strongly with the whistler mode at frequencies near f_{LHR}. Electrostatic instabilities and whistler mode coupling effects of this type have been discussed by several investigators [e.g., *Sizonenko and Stepanov*, 1967; *James*, 1976; *Maggs*, 1976]. Since both the broad-band electrostatic noise and the whistler mode magnetic noise bursts occur in regions with substantial field-aligned currents, it seems almost certain that both of these waves are produced by a current-driven instability. Although several current-driven instabilities are known which could possibly account for these waves [e.g., *Kindel and Kennel*, 1971], further detailed studies

of the charged particle distribution functions are needed to identify the plasma instabilities involved in the generation of these waves.

Since the broad-band electrostatic noise is believed to occur on the same magnetic field lines as the inverted V electron events, it is of interest to consider how this plasma wave turbulence may be associated with the inverted V electron acceleration and heating. As was discussed by *Frank and Ackerson* [1971], *Evans* [1974], and others, the inverted V electron acceleration is believed to take place relatively close to the earth, at radial distances of only a few earth radii. Numerous other phenomena, such as auroral hiss [*Gurnett and Frank, 1972a*] and auroral kilometric radiation [*Gurnett, 1974*], clearly show that some distinctly nonthermal process is taking place along the nighttime auroral field lines at altitudes from about 5,000 to 20,000 km. On the same magnetic field lines as the inverted V events, intense field-aligned currents are known to flow between the distant magnetosphere and the ionosphere, and intense fluxes of protons are detected streaming toward the earth in the distant magnetotail [*Frank et al., 1976*]. In considering the possible role of the plasma wave turbulence detected by Hawkeye 1 and Imp 6 on the acceleration and heating of the auroral particles, two main questions can be identified: (1) whether the waves act to thermalize the earthward streaming protons and in the process heat the electrons to the high temperatures characteristic of the inverted V events, and (2) whether the waves cause an anomalous resistivity sufficiently large to account for field-aligned potential differences thought to be involved in the primary acceleration of the inverted V electrons.

Since only a small fraction of the protons streaming toward the earth in the distant magnetotail are observed to return from the direction of the earth, *Frank* [1972] has suggested that the energy carried by these protons is transferred to the electrons at some point along the magnetic field line closer to the earth, thereby accounting for the inverted V electron precipitation and the absence of comparable intense proton fluxes at low altitudes. Since the plasma at these altitudes is nearly collisionless, some mechanism is needed to transfer the energy and momentum from the electrons to the protons. The occurrence of intense plasma wave turbulence along the field lines where the inverted V events are observed strongly suggests that this turbulence is involved in heating these electrons. In many respects the process could be similar to the earth's bow shock, where plasma waves play the dominant role in the plasma heating. For the observed electric field spectrum the primary interactions with the protons would be expected at the harmonics nf_g^+ of the proton gyrofrequency. The electron heating could occur by either Landau damping or cyclotron damping of the waves generated by the earthward streaming protons.

In addition to the heating caused by the generation and reabsorption of plasma waves, energy exchange can also occur in regions of field-aligned currents because of the anomalous resistivity caused by the plasma wave turbulence. Estimates of the field-aligned potential differences caused by anomalous resistivity in regions of field-aligned currents have been previously given by *Fredricks et al.* [1973]. Assuming an rms broad-band electric field strength of 90 mV m^{-1}, Fredricks et al. estimate that field-aligned potential differences of the order of 2 kV can be expected. In the region surveyed by Hawkeye 1 and Imp 6 the rms electric field strength of the broad-band electrostatic noise is seldom larger than about 10–30 mV m^{-1}, and in the distant magnetotail the electric field strength of this noise is even smaller, seldom exceeding about 1–2 mV m^{-1} [see *Gurnett et al., 1976*]. Since the anomalous resistivity varies as the square of the electric field strength [*Sagdeev and Galeev, 1966*], the field-aligned potential differences in the regions surveyed by Hawkeye 1 and Imp 6 are less than those estimated by Fredricks et al., probably not more than about 200 V, assuming that the other parameters are similar. Potential differences of this order are too small to account for the electron energies of ~10 keV observed in the inverted V electron precipitation at low altitudes. However, it should be noted that the Hawkeye 1 and Imp 6 measurements do not include the radial distance range of about 1.8–4.0 R_E (at L = 8), and the electric field intensity may be significantly larger in this altitude range. Comparisons between Imp 8 and Hawkeye 1 in fact suggest that the electric field intensity of the broad-band electrostatic noise increases at lower altitudes (compare Figure 5 from *Gurnett et al.* [1976] with Figure 6 of this paper). The possibility that the electric field intensities may increase with decreasing altitude is further supported by the Ogo 5 observations of *Scarf et al.* [1973], in which electric field strengths as large as ~200 mV m^{-1} were observed at a radial distance of 2.5 R_E. Broad-band electric field strengths this large have not yet been observed by Hawkeye 1 and Imp 6. The absence of such large field strengths in the Hawkeye 1 and Imp 6 data is not considered to be in disagreement with the Ogo 5 measurements because of the previously mentioned limitations in the orbital coverage, which has not yet provided measurements at radial distances near 2.5 R_E on the auroral field lines. Hopefully, data obtained later in the Hawkeye 1 lifetime can provide the measurements necessary to extend the results of the present study into the region from 1.8 to 4.0 R_E along the auroral field lines.

Since the wavelength of the electric field turbulence detected by Hawkeye 1 and Imp 6 may be very short, consideration must also be given to the possibility that the wavelengths may be shorter than the antenna lengths (42.45 and 92.50 m for Hawkeye 1 and Imp 6, respectively). If wavelengths λ occur which are shorter than the antenna length L, then the electric field strength will be underestimated, possibly by a large factor if $\lambda \ll L$. The shortest wavelength which can occur in a plasma is approximately $\lambda_m = 2\pi\lambda_D = 46.6(T/n)^{1/2}$ m, where λ_D is the Debye length, T is the electron temperature in electron volts, and n is the electron density in units per cubic centimeter. In the high-altitude region ($R > 4.0\ R_E$) surveyed by Hawkeye 1 and Imp 6 a reliable upper limit to the electron density can be obtained from the low-frequency cutoff of the continuum radiation, which must occur at frequencies greater than the local electron plasma frequency $f > f_p^- \simeq 9(n)^{1/2}$ kHz. In the region where the broad-band electrostatic noise is observed the continuum radiation cutoff is typically about 15 kHz and almost never greater than 30 kHz, which implies densities of typically 3 cm^{-3} and almost never more than 10 cm^{-3}. The electron temperature is more difficult to estimate. Because substantial fluxes of electrons with energies of several hundred electron volts are usually present in these regions, it is estimated that the electron temperature is almost certainly of the order of 100 eV or more. When n = 10 cm^{-3} and T = 100 eV, the minimum wavelength is λ_m = 147.4 m, which is longer than either the Hawkeye 1 or the Imp 6 antenna by a significant factor. We conclude that errors due to short wavelength effects are not likely to be present in the high-altitude ($R > 4.0\ R_E$) measurements presented in this paper. This conclusion has been verified in a few cases by comparing measurements obtained with antennas of different lengths on Imp 6, which show the expected proportionality of the signal strength with in-

creasing antenna length which should be observed when $\lambda \gg L$.

For the low-altitude region ($R < 1.8\ R_E$) surveyed by Hawkeye 1 it is certain that the minimum wavelength can be much less than the antenna length because of the larger electron density and lower electron temperature in the ionosphere. Whether the broad-band electric field turbulence detected at low altitudes actually has wavelengths sufficiently short to cause serious errors in the electric field measurements is difficult to determine and has not been investigated in detail, since the primary emphasis of this study has been on the high-altitude observation. On the basis of earlier studies by *Kelley and Mozer* [1972], in which wavelengths of the low-altitude electric field turbulence were directly measured, *Kintner* [1976] has presented arguments showing that the wavelengths of the broad-band electrostatic noise are sufficiently long to preclude the possibility of serious errors in the electric field spectrum even at low altitudes.

Acknowledgments. The Hawkeye 1 program at the University of Iowa is under the supervision of J. A. Van Allen, to whom the authors are further indebted for the magnetic field data used herein. The authors also wish to express their thanks to K. Ackerson, R. Shaw, R. Anderson, R. West, and W. Kurth for their assistance in data processing and the preparation of illustrations. The research at the University of Iowa was supported by the National Aeronautics and Space Administration through grants NGL-16-001-002 and NGL-16-001-043, contracts NAS1-11257 and NAS1-13129 with the Langley Research Center, and contracts NAS5-20539, NAS5-11074, and NAS5-11431 with the Goddard Space Flight Center and by the U.S. Office of Naval Research. The research at the Max-Planck-Institut was supported by the Alexander von Humboldt Foundation.

The Editor thanks R. W. Fredricks and T. Laaspere for their assistance in evaluating this paper.

REFERENCES

Ackerson, K. L., and L. A. Frank, Correlated satellite measurements of low-energy electron precipitation and ground-based observations of a visible auroral arc, *J. Geophys. Res.*, *77*, 1128, 1972.

Aubry, M. P., M. G. Kivelson, R. L. McPherron, C. T. Russell, and D. S. Colburn, Outer magnetosphere near midnight at quiet and disturbed times, *J. Geophys. Res.*, *77*, 5487, 1972.

Carlqvist, P., On the formation of double layers in plasmas, *Cosmic Electrodynamics*, *3*, 377, 1972.

Coroniti, F. V., and C. F. Kennel, Polarization of the auroral electrojet, *J. Geophys. Res.*, *77*, 2835, 1972.

Coroniti, F. V., and C. F. Kennel, Can the ionosphere regulate magnetospheric convection?, *J. Geophys. Res.*, *78*, 2837, 1973.

Evans, D. S., Precipitating electron fluxes formed by a magnetic field aligned potential difference, *J. Geophys. Res.*, *79*, 2853, 1974.

Fairfield, D. H., Magnetic field signatures of substorms on high latitude field lines in the nighttime magnetosphere, *J. Geophys. Res.*, *78*, 1553, 1973.

Frank, L. A., Initial observations of low-energy electrons in the earth's magnetosphere with Ogo 3, *J. Geophys. Res.*, *72*, 185, 1967.

Frank, L. A., Plasma entry into the earth's magnetosphere, in *Critical Problems of Magnetospheric Physics*, edited by E. R. Dyer, p. 35, IUCSTP Secretariat, Washington, D. C., 1972.

Frank, L. A., and K. L. Ackerson, Observations of charged particles precipitated into the auroral zone, *J. Geophys. Res.*, *76*, 3612, 1971.

Frank, L. A., and D. A. Gurnett, Distributions of plasmas and electric fields over the auroral zones and polar caps, *J. Geophys. Res.*, *76*, 6829, 1971.

Frank, L. A., K. L. Ackerson, and R. P. Lepping, On hot tenuous plasmas, fireballs, and boundary layers in the earth's magnetotail, *J. Geophys. Res.*, *81*, 5859, 1976.

Fredricks, R. W., F. L. Scarf, and C. T. Russell, Field-aligned currents, plasma waves, and anomalous resistivity in the disturbed polar cusp, *J. Geophys. Res.*, *78*, 2133, 1973.

Gurnett, D. A., A satellite study of VLF hiss, *J. Geophys. Res.*, *71*, 5599, 1966.

Gurnett, D. A., The earth as a radio source: Terrestrial kilometric radiation, *J. Geophys. Res.*, *79*, 4227, 1974.

Gurnett, D. A., The earth as a radio source: The nonthermal continuum, *J. Geophys. Res.*, *80*, 2751, 1975.

Gurnett, D. A., and L. A. Frank, VLF hiss and related plasma observations in the polar magnetosphere, *J. Geophys. Res.*, *77*, 172, 1972*a*.

Gurnett, D. A., and L. A. Frank, ELF noise bands associated with auroral electron precipitation, *J. Geophys. Res.*, *77*, 3411, 1972*b*.

Gurnett, D. A., and L. A. Frank, Observed relationships between electric fields and auroral particle precipitation, *J. Geophys. Res.*, *78*, 145, 1973.

Gurnett, D. A., and R. R. Shaw, Electromagnetic radiation trapped in the magnetosphere above the plasma frequency, *J. Geophys. Res.*, *78*, 8136, 1973.

Gurnett, D. A., L. A. Frank, and R. P. Lepping, Plasma waves in the distant magnetotail, *J. Geophys. Res.*, *81*, 6059, 1976.

Holzer, T. E., and T. Sato, Quiet auroral arcs and electrodynamic coupling between the ionosphere and the magnetosphere, *J. Geophys. Res.*, *78*, 7330, 1973.

James, H. G., VLF saucers, *J. Geophys. Res.*, *81*, 501, 1976.

Kelley, M. C., and F. S. Mozer, A satellite survey of vector electric fields in the ionosphere at frequencies of 10 to 500 Hz, *J. Geophys. Res.*, *77*, 4158, 1972.

Kindel, J. M., and C. F. Kennel, Topside current instabilities, *J. Geophys. Res.*, *76*, 3055, 1971.

Kintner, P. M., Jr., Observations of velocity shear driven plasma turbulence, *J. Geophys. Res.*, *81*, 5114, 1976.

Kurth, W. S., M. M. Baumback, and D. A. Gurnett, Direction-finding measurements of auroral kilometric radiation, *J. Geophys. Res.*, *80*, 2764, 1975.

Laaspere, T., W. C. Johnson, and L. C. Semprebon, Observations of auroral hiss, LHR noise, and other phenomena in the frequency range 20 Hz to 540 kHz on Ogo 6, *J. Geophys. Res.*, *76*, 4477, 1971.

Maggs, J. E., Coherent generation of VLF hiss, *J. Geophys. Res.*, *81*, 1707, 1976.

McEwen, D. J., and R. E. Barrington, Some characteristics of the lower hybrid resonance noise bands observed by the Alouette 1 satellite, *Can. J. Phys.*, *45*, 13, 1967.

Mozer, F. S., Anomalous resistivity and parallel electric fields, in *Magnetospheric Particles and Fields*, edited by B. M. McCormac, D. Reidel, Dordrecht, Netherlands, in press, 1977.

Papadopoulos, K., and T. Coffey, Anomalous resistivity in the auroral plasma, *J. Geophys. Res.*, *79*, 1558, 1974.

Paschmann, G., G. Haerendel, N. Sckopke, H. Rosenbauer, and P. C. Hedgecock, Plasma and magnetic field characteristics of the distant polar cusp near local noon, *J. Geophys. Res.*, *81*, 2883, 1976.

Russell, C. T., R. E. Holzer, and E. J. Smith, Ogo 3 observations of ELF noise in the magnetosphere, 1, Spatial extent and frequency of occurrence, *J. Geophys. Res.*, *74*, 755, 1969.

Sagdeev, R. Z., and A. A. Galeev, Non-linear plasma theory, *Tech. Rep. IC/66/64*, Int. Center for Theor. Phys., Trieste, Italy, 1966.

Sato, T., alnd T. E. Holzer, Quiet auroral arcs and electrodynamic coupling between the ionosphere and the magnetosphere, 1, *J. Geophys. Res.*, *78*, 7314, 1973.

Scarf, F. L., R. W. Fredricks, I. M. Green, and C. T. Russell, Plasma waves in the dayside polar cusp, *J. Geophys. Res.*, *77*, 2274, 1972.

Scarf, F. L., R. W. Fredricks, C. T. Russell, M. Kivelson, M. Neugebauer, and C. R. Chappell, Observation of a current-driven plasma instability at the outer zone–plasma sheet boundary, *J. Geophys. Res.*, *78*, 2150, 1973.

Scarf, F. L., R. W. Fredricks, C. T. Russell, M. Neugebauer, M. Kivelson, and C. R. Chappell, Current-driven plasma instabilities at high latitudes, *J. Geophys. Res.*, *80*, 2030, 1975.

Shaw, R. R., and D. A. Gurnett, Electrostatic noise bands associated with the electron gyrofrequency and plasma frequency in the outer magnetosphere, *J. Geophys. Res.*, *80*, 4259, 1975.

Sizonenko, V. L., and K. N. Stepanov, Plasma instability in the electric field of an ion-cyclotron wave, *Nucl. Fusion*, *7*, 131, 1967.

Taylor, W. W. L., and S. D. Shawhan, A test of incoherent Cerenkov radiation for VLF hiss and other magnetospheric emissions, *J. Geophys. Res.*, *79*, 105, 1974.

(Received April 29, 1976;
accepted September 17, 1976.)